PCCP

Accepted Manuscript

This article can be cited before page numbers have been issued, to do this please use: F. M. Cabrerizo, F. A. O. Rasse-Suriani, M. P. Denofrio, J. G. Yañuk, M. M. Gonzalez, E. Wolcan, M. Seifermann and R. Erra-Balsells, *Phys. Chem. Chem. Phys.*, 2015, DOI: 10.1039/C5CP05866J.

ROYAL SOCIETY OF CHEMISTRY

www.rsc.org/pccp

View Article Online
DOI: 10.1039/C5CP05866J

CHEMICAL AND PHOTOCHEMICAL PROPERTIES OF CHLOROHARMINE DERIVATIVES IN AQUEOUS SOLUTIONS

Federico A. O. Rasse-Suriani[a,‡], *M. Paula Denofrio*[a,‡], *Juan G. Yañuk*[a], *M. Micaela Gonzalez*[a], *Ezequiel Wolcan*[b], *Marco Seifermann*[c], *Rosa Erra-Balsells*[d,*] *and Franco M. Cabrerizo*[a,*]

[a] Instituto de Investigaciones Biotecnológicas - Instituto Tecnológico de Chascomús (IIB-INTECH), Universidad Nacional de San Martín (UNSAM) - Consejo Nacional de Investigaciones Científicas y Técnicas (CONICET), Av. Intendente Marino Km 8.2, CC 164 (B7130IWA), Chascomús, Argentina. E-mail: fcabrerizo@intech.gov.ar

[b] Instituto de Investigaciones Fisicoquímicas Teóricas y Aplicadas (INIFTA, UNLP, CCT La Plata-CONICET), Diag. 113 y 64, Sucursal 4, C.C. 16, (B1906ZAA) La Plata, Argentina.

[c] Institute of Pharmacy and Biochemistry, University of Mainz, Staudingerweg 5, Mainz, Germany.

[d] CIHIDECAR - CONICET, Departamento de Química Orgánica, Facultad de Ciencias Exactas y Naturales, Universidad de Buenos Aires, Pabellón 2, 3p, Ciudad Universitaria, (1428) Buenos Aires, Argentina. E-mail: erra@qo.fcen.uba.ar

‡ These authors contributed equally.

* To whom correspondence should be addressed (fcabrerizo@intech.gov.ar and erra@qo.fcen.uba.ar)

View Article Online
DOI: 10.1039/C5CP05866J

ABSTRACT

Thermal and photochemical stability (Φ_R), room temperature UV-vis absorption and fluorescence spectra, fluorescence quantum yields (Φ_F) and lifetimes (τ_F), quantum yields of hydrogen peroxide (Φ_{H2O2}) and singlet oxygen (Φ_Δ) production, and triplet lifetimes (τ_T) have been obtained for the neutral and protonated forms of 6-chloroharmine, 8-chloroharmine and 6,8-dichloroharmine, in aqueous media. When it was possible, the effect of pH and oxygen concentration was evaluated. The nature of electronic transitions of protonated and neutral species of the three investigated chloroharmines were established by Time-Dependent Density Functional Theory (TD-DFT) calculations. The impact of all the foregoing observations on the biological role of the studied compounds is discussed.

View Article Online
DOI: 10.1039/C5CP05866J

INTRODUCTION

β-Carbolines (βCs) are a group of alkaloids present in a wide range of species that are different from a phylogenetic point of view such as mammals,[1-5] plants,[6-8] arthropods,[9] insects,[10] etc. Although the great majority of βCs described do not contain halogen atoms in their structure, recently, more than forty halogenated-βCs have been isolated from sea invertebrates, algae, cyanobacteria and other organisms.[11-13]

Ascidia *Eudistoma olivaceum* (from the Caribbean Sea) contains some halogenated full-aromatic βCs such as Eudistomin N (6-bromo-9*H*-pyrido[3,4-*b*]indole or 6-bromo-norharmane) and Eudistomin O (7-bromo-9*H*-pyrido[3,4-*b*]indole or 7-bromo-norharmane),[14-16] among others. Ascidia *Eudistoma fragum* (from coastal zone of New Caledonia) contains other non-full aromatic bromine derivatives ((1R)-6-bromo-2-methyl-1-[(2S)-1-methyl-2-pyrrolidinyl]-2,3,4,9-tetrahydro-1*H*-pyrido[3,4-*b*]indole, or woodinine).[17, 18] Hydroid *Aglaophenia pluma* produces 6-bromo-1-ethyl-9*H*-pyrido[3,4-*b*]indole (or 6-bromo-1-ethyl-norharmane), 6-bromo-1-methyl-9*H*-pyrido[3,4-*b*]indole (or 6-bromo-1-methyl-norharmane or 6-bromo-harmane), 6,8-dibromo-1-ethyl-9*H*-pyrido[3,4-*b*]indole (or 6,8-dibromo-1-ethyl-norharmane), among others.[19] Chlorinated βC derivatives were also found in various species. Chloro-nostocarboline (or 6-chloro-2-methyl-norharmanium) was found in *Nostocales* (cyanobacteria spread in Europe, Southwest Asia, Australia and New Zealand) and other phototrophic organisms.[11] Bauerine alkaloids A (or 7-chloro-9-methyl-2*H*-pyrido[3,4-*b*]indole), B (or 7,8-dichloro-9-methyl-2*H*-pyrido[3,4-*b*]indole) and C (or 7,8-dichloro-1-hydroxy-9-methyl-2*H*-pyrido[3,4-*b*]indole) were isolated from *Dichotrix baueriana* (a terrestrial blue-green alga).[20]

These halogenated-βCs have been described as bioactive compounds. *In vitro*, they have shown antimicrobial activity against parasites, viruses, yeasts and bacteria.[11, 15, 16, 21] Some halogenated-βCs have a high cytotoxic activity against various cancer cell-lines[22] and some chlorinated-derivatives were suggested as potent and selective synthetic kinase inhibitors.[23] Despite their abundance, the main biological role of these alkaloids as well as many fundamental aspects of the mechanisms involved still remain poorly understood; as consequence the potential use of synthetically modified (halogenated) βCs still is not clearly known. Moreover, taking into account that non-halogenated βCs are photoactive compounds[24-30] and having in mind their abundance in nature (including phototrophic organisms),[11] the photochemical and photobiological properties of halogenated-βCs deserve to be explored in detail.

Tarzi *et. al.*[31-33] described the effect of chlorine and bromine atoms as substituents on the UV-vis absorption and fluorescence emission spectra of norharmane, harmane and harmine in organic solvents (ethanol and acetonitrile). However, studies in water environment, which are

View Article Online
DOI: 10.1039/C5CP05866J

relevant from the biological point of view, were not attempted. Very recently, we have described the spectroscopic and fluorescence behaviour of three protonated chloroharmines (*i.e.*, in acidic aqueous solutions and in acetonitrile/TFA) upon one- and two-photon excitation.[34] Briefly, solvent-dependent behaviour on the one- and two-photon absorption spectra of protonated chloroharmines was observed. As it was expected, chlorine atoms introduce quite strong changes on the electronic distribution (on both ground and excited states) of the βC ring. However, having in mind the well-known dependence of the physicochemical and photochemical properties of other related βCs on the pH and oxygen concentration,[35-38] the effect of these environmental conditions still need to be addressed for chloroharmines. Moreover, no information is available in the literature regarding the chemical (thermal) and photochemical stability of chlorinated-βCs.

In the following sections we describe different aspects related to the physicochemical and photochemical properties of three chloro-substituted βCs obtained from 7-methoxy-1-methyl-9*H*-pyrido[3,4-*b*]indole (harmine, Ha): 6-chloroharmine (6-Cl-Ha), 8-chloroharmine (8-Cl-Ha) and 6,8-dichloroharmine (6,8-diCl-Ha), in aqueous media (Scheme 1). These compounds might serve as representative examples of other naturally occurring βCs. On the other hand, studies on synthetic chloro-βCs are also relevant from the biotechnological point of view (*i.e.*, development of novel antimicrobial and/or photosensitizing agents).

The study started by outlining the pH effect on the spectroscopy and also on the chemical and photochemical stability of the three investigated compounds. Reactive oxygen species produced upon one-photon excitation are monitored and quantified and the role of oxygen and its highly reactive species on the photochemistry of chloroharmines is investigated. The impact of all the foregoing observations on the biological role of the studied compounds is discussed.

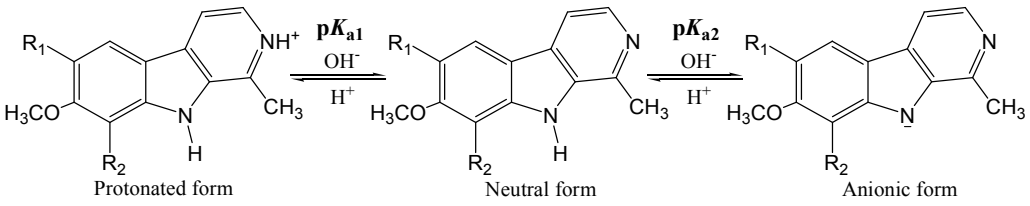

	R_1	R_2
Harmine (**Ha**)	-H	-H
6-Chloro-harmine (**6-Cl-Ha**)	-Cl	-H
8-Chloro-harmine (**8-Cl-Ha**)	-H	-Cl
6,8-diChloro-harmine (**6,8-diCl-Ha**)	-Cl	-Cl

Scheme 1. Structures of chloroharmines studied and acid-base equilibria present in aqueous solution, in the pH range 2-13.

EXPERIMENTAL

β-Carbolines. 7-Methoxy-1-methyl-9*H*-pyrido[3,4-*b*]indole (harmine, Ha) (> 98%) from Sigma-

View Article Online
DOI: 10.1039/C5CP05866J

Aldrich was used without further purification. The method used to synthesize and purify chloroharmine derivatives has been published elsewhere.[39]

pH adjustment. The pH of the solutions was adjusted by adding drops of aqueous NaOH or HCl solutions (concentration ranged from 0.1 M to 2.0 M) with a micropipette. When solutions free of chloride ion were needed, $HClO_4$ was used for acidification. The ionic strength was approximately 10^{-3} M in all the experiments. In experiments using D_2O as solvent, D_2O (> 99.9%; Sigma), DCl (99.5%; Aldrich) in D_2O, and NaOD (Aldrich) in D_2O were used. The pD of the solution was adjusted as it was described elsewhere,[33] the final isotope purity was greater than 96%.

Dissolved oxygen concentration. Chloroharmines aqueous solutions were equilibrated (saturated) to three different ambient oxygen partial pressure conditions by bubbling nitrogen (or argon), air, and oxygen through the solution, for approximately 20 min, leading to a dissolved oxygen concentration ($[O_2]$) of 0, 0.28 and 1.33 mM, respectively.

Elapsed irradiation. Aqueous βC solutions were irradiated at 350 nm or 365 nm, in 1 cm quartz cells at room temperature with a Rayonet RPR lamp (bandwidth ~15 nm, Southern N.E. Ultraviolet Co.). Experiments were performed in the presence and absence of air. Oxygen-free solutions were obtained by bubbling with Ar or N_2 gas for 20 min.

UV/vis Analysis and pK_a measurement. Electronic UV-vis absorption spectra were recorded on Shimadzu PC2101 and Perkin-Elmer λ-25 spectrophotometers. Measurements were made using 1 cm path length quartz cuvettes, at room temperature. pK_a values were determined from absorption changes following the procedure described elsewhere.[40]

High-Performance Liquid Chromatography (HPLC). A Waters 1525 binary Pump controller with a Waters 2475 multi-λ fluorescence detector was used to monitor and quantify the photochemical reactions. Aqueous solutions of commercial standards were employed for the calibration curves. Stationary phase: GracePrevail C18 (250 × 4.6 mm, 5 μm). Mobile phase: 50/50 (v/v) mixture of formic acid aqueous solution (0.08% (v/v), pH 3.2) and MeOH. Flow rate: 1 mL / min.

Determinations of quantum yield of chloroharmine consumption. Quantum yields of reactant disappearance (Φ_R) were obtained using the following equation:

$$\Phi_R = - \frac{(d[R]/dt)_0}{q_{n,p,\lambda}} \qquad (1)$$

where $(d[R]/dt)_0$ is the initial rate of reactant consumption and $q_{n,p,\lambda}$ is the number of photons of the excitation wavelength λ, per time interval (spectral photon flux, amount basis) absorbed by the reactant per volume, V. For determining the consumption rate, experiments were carried out using

View Article Online
DOI: 10.1039/C5CP05866J

solutions with an initial reactant concentration of ~150 μM (except for Ha at pH 10.0 where ~30 μM was used). Under these conditions, the time evolution of the reactant concentration followed a zero-order rate law over a period of time within which the change of $q_{n,p,\lambda}$ was negligible. In our experiments, this condition was fulfilled at irradiation times less than 120 min. The initial rates were obtained from the slope of the corresponding plots of concentration *vs.* irradiation time within this time window.

Aberchrome 540 (Aberchromics Ltd.) was used as actinometer for the measurements of the incident photon flux at the excitation wavelength (*i.e.*, $q^0_{n,p,\lambda}$ according to Braslavsky *et. al.*).[41] The general approach used is described in detail elsewhere.[35, 42] Values of the photon flux absorbed ($q_{n,p,\lambda}$),[41] were calculated from $q^0_{n,p,\lambda}$ according to the Lambert-Beer law:

$$q_{n,p,\lambda} = q^0_{n,p,\lambda} (1 - 10^{-A}) / V \qquad (2)$$

where A is the absorbance of the sensitizer at the excitation wavelength.

Detection and quantification of H_2O_2. For the determination of H_2O_2, a Cholesterol Kit (Wiener Laboratories S.A.I.C.) was used. H_2O_2 was quantified after reaction with 4-aminophenazone and phenol.[35, 43] Briefly, 600 μl of irradiated solution (UVA) was added to 1.6 ml of reagent. The absorbance at 505 nm of the resulting mixture was measured after 30 min at room temperature, using the reagent as a blank. Aqueous H_2O_2 solutions prepared from commercial standards were employed for obtaining the corresponding calibration curves.

Detection and quantification of chloride ion. A chloride ion-selective electrode Weiss Research RCL3001 was used for monitoring the chloride ion release during both thermal and photochemical reactions studied. The electrode was used following the specifications of the fabricant. Several NaCl solutions (0 ppm - 100 ppm of Cl^-), prepared from a chloride standard solution (1000 ppm, WE-2815, Weiss Res. Inc.), were used for electrode calibration. The ionic strength of samples and standard solutions was adjusted by adding 0.1 M of $NaNO_3$ (from a 5 M stock solution, WE-2510, Weiss Res. Inc.).

Fluorescence emission. Steady-state fluorescence measurements were performed using a Fluoromax4 (HORIBA Jobin Yvon), whereas a single-photon-counting equipment FL3 TCSPC-SP (HORIBA Jobin Yvon) spectrofluorometer was used for time-resolved measurements. Corrected fluorescence spectra were recorded in a 1 cm path length quartz cell at room temperature.

Fluorescence quantum yields (Φ_F) were determined from the corrected fluorescence spectra, integrated over the entire emission profile and were calculated as the average of Φ_F values obtained using different excitation wavelengths over the entire range of the lowest-energy absorption band.

View Article Online
DOI: 10.1039/C5CP05866J

The standard used was quinine sulfate at pH 4 ($\Phi_F = 0.52 \pm 0.02$).[44] To avoid inner filter effects, the absorbance of the solutions at the excitation wavelength was kept below 0.10.

Nanosecond Time-Resolved Experiments. (i) Quantum yields of photosensitized singlet oxygen production, Φ_Δ, were obtained using a pulsed Nd:YAG laser as the excitation source (λ = 355 nm), looking at the 1270 nm $^1O_2$ phosphorescence with a cooled germanium detector.[36] Experiments were performed by comparing the magnitude of the integrated time-resolved phosphorescence signal produced upon one-photon irradiation of the molecule under study to that obtained upon one-photon irradiation of a standard sensitizer (perinaphthenone-2-sulfonic acid (PNS) in deuterated water with $\Phi_\Delta = 0.97 \pm 0.05$[45]).[46] *(ii)* Triplet state kinetics were studied in a pump-probe experiment using instruments and an approach that have likewise been previously described.[37] Typically, chloroharmine acidic aqueous solutions (200 μM) were irradiated at 355 nm. The absorption of the resultant triplet state was probed using the output of a steady-state 200W xenon lamp that had been passed through a water filter to remove the IR-components. The light from the xenon lamp transmitted through the sample was dispersed by a grating onto a PMT (Hamamatsu R928). A filter was inserted to remove residual scattered laser light. The resulting time-resolved signal was digitized and monitored with an oscilloscope (Tektronix TDS5032B). Changes in the amount of transmitted light were monitored at 450 nm where the protonated species of chloroharmine triplet state absorbance is strong.

Computational methods. The electronic structure of the chloroharmine derivatives were determined using tools of Density Functional Theory (DFT)[47-49] as implemented in Gaussian 09 package.[50] Their vacuum geometries were optimized at the B3LYP/TZVP level of theory. Vibrational frequencies were computed at the same level of theory to confirm that these structures were minima on the energy surfaces. The vertical transition energies were calculated at the optimized ground-state geometry by Time-Dependent Density Functional Theory (TD-DFT)[51-53] using B3LYP hybrid functional and aug-cc-pVDZ basis set including solvent effects (water) through the Polarizable Continuum Model[54-56] to produce a number of 110 singlet-to-singlet transitions. Percentage compositions of different molecular fragments to molecular orbitals (MOs) from output files generated from Gaussian 09 were calculated using the AOMix program.[57, 58]

Absorption spectra were simulated with Gaussian distributions with a full-width at half-maximum (fwhm) set to 3000 cm^{-1} with the aid of GaussSum 2.2.5 program. Convoluted spectra are obtained by summing Gaussian functions centred at each calculated wavelength with the maxima related to the value of the oscillator strengths (which are also plotted) using equation 3:[59]

View Article Online
DOI: 10.1039/C5CP05866J

$$\varepsilon(\tilde{\upsilon}) = \frac{2.175\text{x}10^{8}\, Lmol^{-1}cm^{-2}}{\Delta_{½}\tilde{\upsilon}}\left(f_{\text{osc}}\right)\exp\left[-2.772\left(\frac{\tilde{\upsilon}-\tilde{\upsilon}_{i\rightarrow f}}{\Delta_{½}\tilde{\upsilon}}\right)^{2}\right] \quad (3)$$

where, $\Delta_{½}\tilde{\upsilon}$ is the parametrical value of the fwhm of the band (in cm^{-1}), f_{osc} is the oscillator strength and $\tilde{\upsilon}_{i\rightarrow f}$ is the frequency (in cm^{-1}) corresponding to the wavelength of the calculated electronic transition.

RESULTS

Determination of pK_a values

In the pH range 2-13, βCs show two acid-base equilibria (Scheme 1).[35, 38] We report herein the corresponding pK_a values (Table 1) for the three chloroharmine derivatives, assessed using UV-vis spectroscopy. Spectra and titration curves are shown as Electronic Supplementary Information (Figures ESI.1 to ESI.3). It is worth mentioning that 6-Cl-Ha showed a reversible acid-base equilibrium in the pH range 2-10.5 whereas an irreversible chemical reaction was observed under higher alkaline conditions, *i.e.*, pH > 11.2 (see red line in Figure ESI.1a). Irreversible reactions were also observed for 8-Cl-Ha and 6,8-diCl-Ha when were subject to alkaline conditions, even at pH ~8, (*vide infra*). Thus, pK_{a1} values were found to be 6.3 ± 0.2, 6.4 ± 0.2 and 5.4 ± 0.4, for 6-Cl-Ha, 8-Cl-Ha and 6,8-diCl-Ha, respectively. On the other hand, pK_{a2} was only determined for 6-Cl-Ha (10.5 ± 0.3) due to the quite fast chemical reaction followed by neutral and/or anionic species of 8-Cl-Ha and 6,8-diCl-Ha under alkaline conditions (*vide infra*).

The latter data evidences that chlorine atom increases the acidity of the βC moiety: *i.e.*, chloroharmines showed pK_a values lower than Ha (the unsubstituted βC ring) and other related βCs.[35, 60] Note that pK_{a1} values obtained herein are lower than those reported in the literature (8.3 and 8.5 for 6-Cl-Ha and 8-Cl-Ha, respectively).[32] However, the chlorine-atom effect on other βCs described (norharmane and harmane) showed the decrease of their basic character, matching these results with the chlorine-atom-effect on proton affinity (PA) predicted by calculation for ground-state chloro-βCs, including chloroharmines.[32] These facts support the trend of pK_a values measured for chloroharmines in the present work.

Thermal stability of acidic and alkaline solutions

The chemical stability of acidic and alkaline aqueous solutions of three chloroharmines (Scheme 1) was studied using UV-vis spectroscopy for monitoring. Briefly, all the investigated compounds remained stable after 50 days storage in acidic (2 < pH < 5) solution in the dark;

View Article Online
DOI: 10.1039/C5CP05866J

whereas alkaline (pH > 7.4) solutions of the three chloroharmines, kept in the dark, showed irreversible chemical reactions (Figures ESI.1a-3a and ESI.4). Previously, it has been shown that both protonated and neutral chloroharmines were stable when stored in ethanolic solutions.[32] These results show the strong structure and solvent-dependent chemical properties of βCs.

The rate of the irreversible thermal reaction observed strongly depends on the chloroharmine derivative structure (6,8-diCl-Ha > 8-Cl-Ha >>> 6-Cl-Ha). In particular, more than 50% of the two former βCs were consumed during the first 10 min of reaction; whereas hardly any significant UV-vis change was observed when 6-Cl-Ha alkaline (pH 8) solutions were incubated for more than 30 min, at room temperature (data not shown). The short distance between the chlorine atom and the indolic-NH group in 8-chloro-substituted βCs, would account for the formation of a hydrogen-bridge-like-interaction.[32] That would be a reasonable explanation for the higher rate of reaction (probably hydrolysis-like reaction) observed when 8-Cl-Ha and 6,8-diCl-Ha are kept in alkaline aqueous solutions.

According to the UV-vis spectra (Figures ESI.1a-3a and ESI.4), the nature of the product/s of the thermal reaction is βC-like because the main absorption band, centred at ~360 nm, remains present in all cases. The latter fact is in agreement with a nucleophilic substitution of the chlorine atom by a hydroxyl group and/or a βC dimerization-like reaction (*vide infra*). This hypothesis should be further investigated.

UV-vis absorption spectra

We conducted experiments with Cl-βCs solutions at two different pH-ranges (3.0 - 4.0 and 8.0 - 9.0) where protonated and neutral form, respectively, are the dominant species (Scheme 1). The corresponding experimental UV-vis absorption spectra are shown in Figure 1. For comparative purposes, the corresponding absorption spectra of Ha were also included.

Data reported herein show both similarities and remarkable differences with those reported for chloroharmines in ethanolic solutions.[32] Briefly, *(i)* in the range 200 - 500 nm, all compounds show three absorption bands. Table 1 collects relevant data for the electronic transitions $S_0 \rightarrow S_1$ and $S_0 \rightarrow S_2$, located in the 320 - 400 region and in the 275 - 320 region, respectively. *(ii)* The relative spectral behaviour observed for the protonated and neutral species of each compound was similar to that observed in organic protic solvents (*i.e.*, ethanol). The protonated species show bathochromic shifts and hyperchromicity in their absorption bands with respect to the corresponding neutral species. *(iii)* With respect to Ha, protonated chloroharmines show a clear bathochromic shift of the lowest absorption band ($S_0 \rightarrow S_1$) and a hypsochromic shift of the $S_0 \rightarrow S_2$ transition band (with the

View Article Online
DOI: 10.1039/C5CP05866J

exception of 8-Cl-HaH$^+$). *(iv)* The chlorine atom on neutral species induces a clear effect only on the lowest energy absorption band: the $S_0 \rightarrow S_1$ transition of the three chloroharmines investigated are red-shifted with respect to Ha, whereas the maximum of absorption of the other electronic transitions showed no significant differences.[61] *(v)* On the contrary to what was observed in organic protic solvents, the presence of a chlorine atom at position C-6 of the protonated βC ring prompts a better resolution of the absorption bands (*i.e.*, transitions $S_0 \rightarrow S_1$ and $S_0 \rightarrow S_2$, in 6-Cl-Ha and 6,8-diCl-Ha).

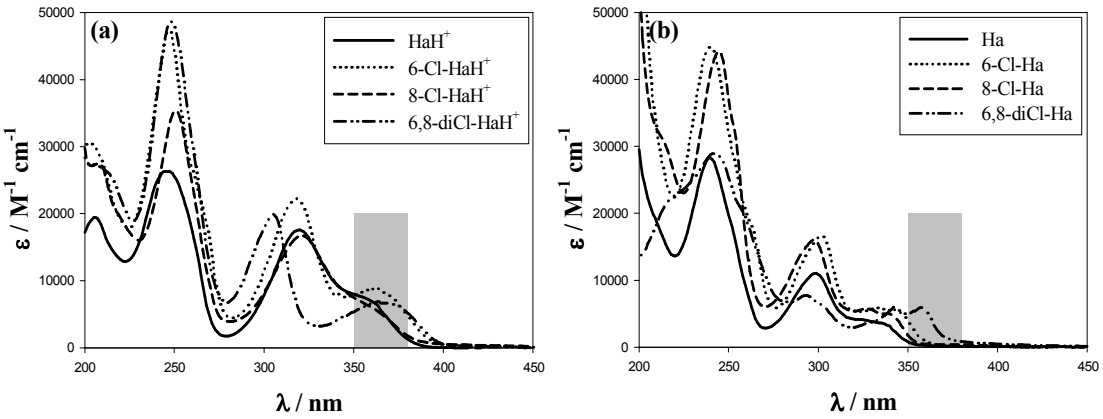

Figure 1. UV-vis absorption spectra of protonated **(a)** and neutral **(b)** species of the investigated Cl-βCs recorded in aqueous solutions. Grey bar depicts the irradiation range (*i.e.*, 365 ± 15 nm) in photostability experiments conducted.

Computational analysis

TD-DFT calculations were performed on different geometry optimized structures corresponding to the existing species in aqueous solutions to better understand the substituent and protonation effects on the photophysical properties of the chloroharmine derivatives. In the following section, TD-DFT results corresponding to the two lowest energy bands of the chloroharmine derivatives will be discussed in detail, as the electronic transitions in this near UV-vis energy region are the ones responsible of the observed fluorescence and the photochemical properties. The calculated TD-DFT results are summarized and compared with experimental data for 6-Cl-Ha, 8-Cl-Ha, 6,8-diCl-Ha and their corresponding protonated analogues (Table 1, entries 4, 6 and 7). It is observed that the main spectral features are predicted to a great accuracy, both in position and relative intensities, by TD-DFT calculations. The main molecular orbitals (MOs) involved in the $S_0 \rightarrow S_1$ and $S_0 \rightarrow S_2$ electronic transitions are the highest occupied MO (HOMO, H), the lowest unoccupied MO (LUMO, L) and the second highest occupied MO (H–1). The second lowest unoccupied MO (L+1) makes only minor contributions to those electronic transitions. For all the compounds, with the exception of 8-Cl-HaH$^+$, the first excited state, which corresponds to a $S_0 \rightarrow S_1$ electronic transition, is predominantly a H→L transition.[62] The second excited state, $S_0 \rightarrow S_2$,

View Article Online
DOI: 10.1039/C5CP05866J

corresponds to a H–1→L transition. 8-Cl-HaH$^+$ is an exception, since the $S_0 \rightarrow S_1$ electronic transition corresponds to a H–1→L transition and $S_0 \rightarrow S_2$ electronic transition is of H→L nature.

Figures 2 and 3 show spatial plots of those MOs, which provide interesting insights to the electronic transitions of protonated and neutral chloroharmines, respectively. We give below a description of H–1, H and L MOs of chloroharmine derivatives based on Figures 2 and 3:

6-Cl-Ha and 8-Cl-Ha. H has a significant amount of electron density on the chlorine atom as well as on the pyrrolic NH. The electron density over the chlorine atom and pyrrolic NH is lower in H–1 than in H. However, the electron density residing in O-CH_3 substituent is higher in H–1 than in H. On the other hand, L orbital has very little electron density on both chlorine atom and pyrrolic NH (at an isocontour value of 0.02 no electron density is observed on Cl of 6-Cl-Ha), while the electron density over O-CH_3 substituent is of comparable amount for L and H. Furthermore, the amount of electron density over pyridinic N is higher in L than in H or H–1.[62]

6.8-diCl-Ha. H and H–1 have a significant amount of electron density on both chlorine atoms. While H has a significant amount of electron density over pyrrolic NH, H–1 has not. The electron density over O-CH_3 substituent is significant in H–1 while it is nil (at an isocontour value of 0.02) for H. Furthermore, the amount of electron density over pyridinic N is higher in L than in H, though in L it is comparable to that of H–1.[63] The amount of electron density over 8-Cl is lower in L than in both H and H-1 while the electron density over 6-Cl is nil in L. Similar conclusions can be made from Figure 2 based on the relative electron density contributions of Cl, pyrrolic NH, pyridine NH$^+$ and O-CH_3 to H-1, H and L MOs of 6-Cl-HaH$^+$, 8-Cl-HaH$^+$ and 6,8-diCl-HaH$^+$.

With the aid of AOMIX program, which takes advantage of Mulliken population analysis to get information on electronic structure of molecules, we calculated the orbital percentage composition of the relevant MOs based on the contributions of the different fragments in which the whole molecule can be split for analysis. The following fragments were defined: (i) pyridinic nitrogen (N or NH$^+$ in case of protonated chloroharmines), (ii) NH of pyrrolic ring, (iii) Cl substituent on 6 and/or 8 position, (iv) CH_3 substituent, (v) O-CH_3 substituent (vi) phenyl ring (without Cl and O-CH_3 substituents) and (vii) pyridine ring (excluding N). Table ESI.1 (see Supplementary Information) lists the orbital percentage composition of the relevant MOs of chloroharmine derivatives based on the fragments defined above. Inspection to Table ESI.1 gives a more precise description of electronic transitions than the one that can be inferred from visual inspection of MOs plots as it helps, in addition, to understand electron density differences in MOs aromatic rings. In this regard, in 6-Cl-Ha, 8-Cl-Ha and 6,8-diCl-Ha there is a higher amount of electron density on the pyridine ring in L than in H. In 6-Cl-HaH$^+$, 8-Cl-HaH$^+$ and 6,8-diCl-HaH$^+$, however, the electron density over the phenyl ring is substantially higher in H than in L while the

View Article Online
DOI: 10.1039/C5CP05866J

electron density over the pyridine ring is substantially higher in L than in H. Based on both Figures 2 and 3 and Table ESI.1, in 6-Cl-Ha, 8-Cl-Ha and 6,8-diCl-Ha compounds H→L transition can be visualized as an electronic transition where electron density moves from NH of pyrrolic ring and Cl towards N of pyridine ring and phenyl ring. On the other hand, for 6-Cl-HaH$^+$ and 8-Cl-HaH$^+$ compounds H→L transition involves the transfer of electron density from NH of pyrrolic ring, Cl, O-CH_3 and phenyl ring towards NH$^+$ and the rest of pyridine ring. In 6,8-diCl-HaH$^+$ H→L transition involves the transfer of electron density from NH of pyrrolic ring, Cl and phenyl ring towards NH$^+$ and the rest of pyridine ring. Alternatively, for 6-Cl-Ha, 8-Cl-Ha and 6,8-diCl-Ha compounds H–1→L transition can mainly be viewed as an electronic transition where electron density is transferred from O-CH_3 and phenyl ring towards N and the rest of pyridine ring. For 6-Cl-HaH$^+$, H–1→L is an electronic transition where the electron density is transferred from NH of pyrrolic ring, O-CH_3 and phenyl ring towards NH$^+$ and the rest of pyridine ring. In 8-Cl-HaH$^+$ H–1→L transition is an electronic transition where the electron density is transferred from NH of pyrrolic ring and phenyl ring towards NH$^+$ and the rest of pyridine ring. Finally, in 6,8-diCl-HaH$^+$ H–1→L transition is an electronic transition where the electron density is transferred from both Cl atoms, O-CH_3 and phenyl ring towards NH$^+$ and the rest of pyridine ring.

In previous work the electronic structures of protonated species of chloroharmines were determined using TD-DFT at the CAM-B3LYP/aug-cc-pVDZ/Polarizable Continuum Model level of theory. When comparing the absolute positions of the bands with the experiment it was found that the calculated electronic transitions were blue shifted by 0.5-0.6 eV relative to the experimental absorption bands.[34] In this paper we decided to study the electronic structure of neutral and protonated species of chloroharmines at the B3LYP/aug-cc-pVDZ/PCM level of theory. Figure 4 shows, as a representative example, data obtained for 6-Cl-Ha (results for other two compounds are presented as Supplementary Information in Figures ESI.5 and ESI.6). Calculated electronic spectra, obtained by using equation 3, are simulated from the theoretical results for comparison with experimental data. The comparison between calculated electronic transitions and experimental data improves substantially when using the B3LYP functional instead of CAM-B3LYP (Table 1, entries 3-6). Indeed, the main spectral features are predicted to a great accuracy, both in position and relative intensities,[64] by TD-DFT calculations at the B3LYP/aug-cc-pVDZ/PCM level of theory.

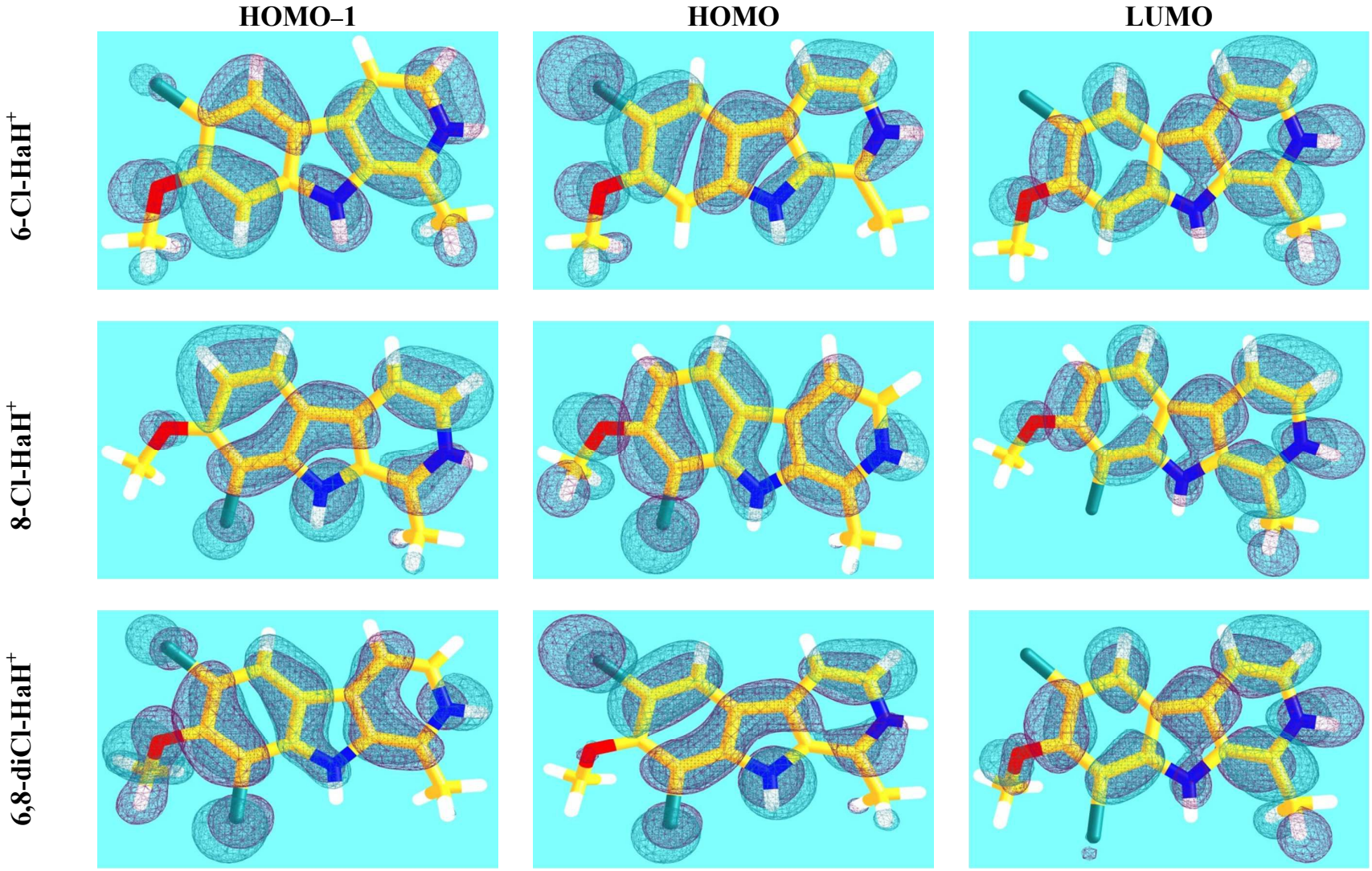

Figure 2: Frontier orbital diagram for 6-Cl-HaH$^+$, 8-Cl-HaH$^+$ and 6,8-diCl-HaH$^+$ compounds (isocontour value = 0.02). H→ L and H–1→ L are the main transitions involved in the low energy absorption bands of the compounds in H_2O in the 300 - 350 nm wavelength region. The vertical transition energies were calculated at the optimized ground-state geometry by TD-DFT calculations (see text for details).

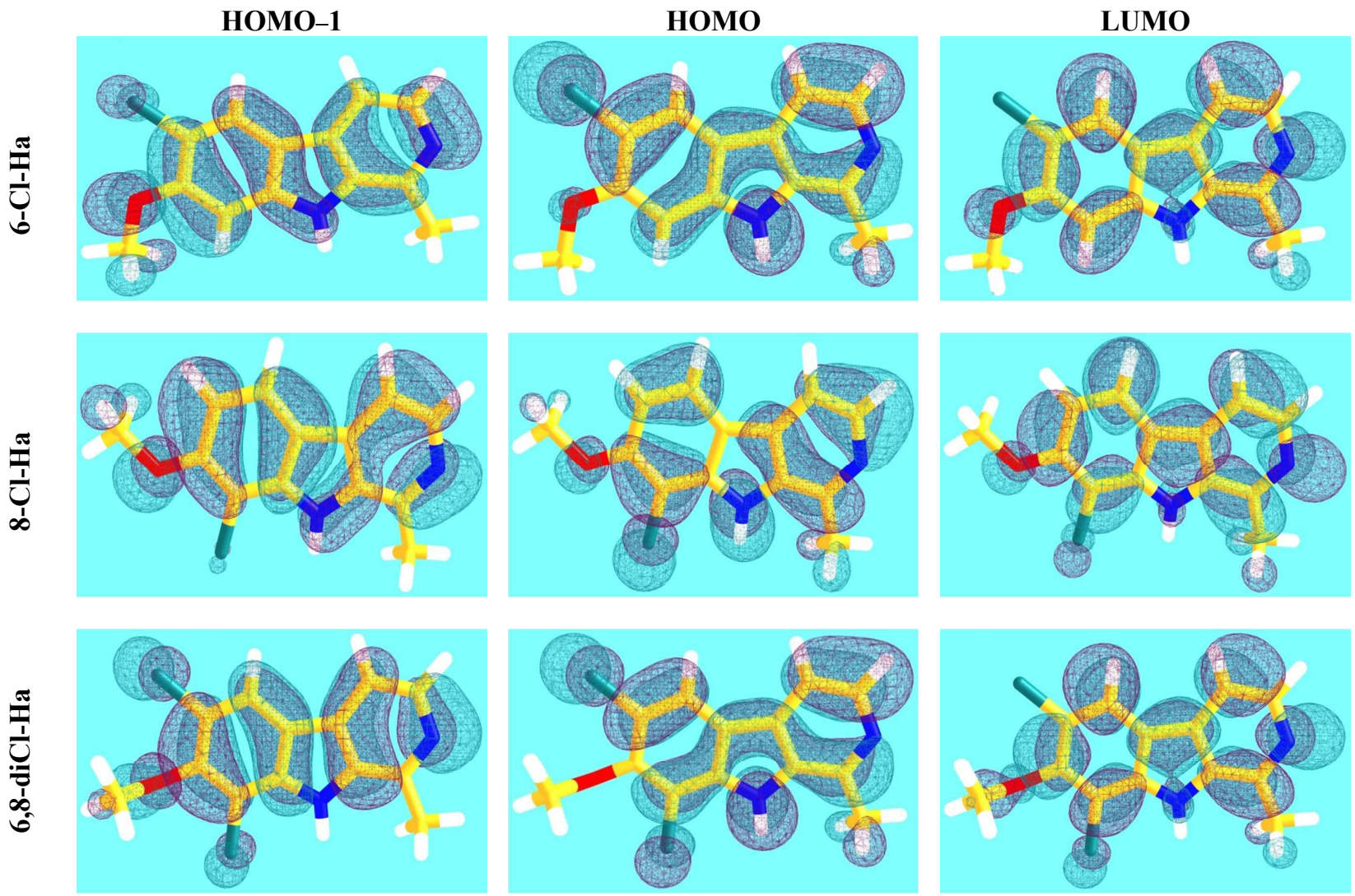

Figure 3: Frontier orbital diagram for 6-Cl-Ha, 8-Cl-Ha and 6,8-diCl-Ha compounds (isocontour value = 0.02). H→ L and H–1→ L are the main transitions involved in the low energy absorption bands of the compounds in H_2O in the 300 - 350 nm wavelength region. The vertical transition energies were calculated at the optimized ground-state geometry by TD-DFT calculations (see text for details).

View Article Online
DOI: 10.1039/C5CP05866J

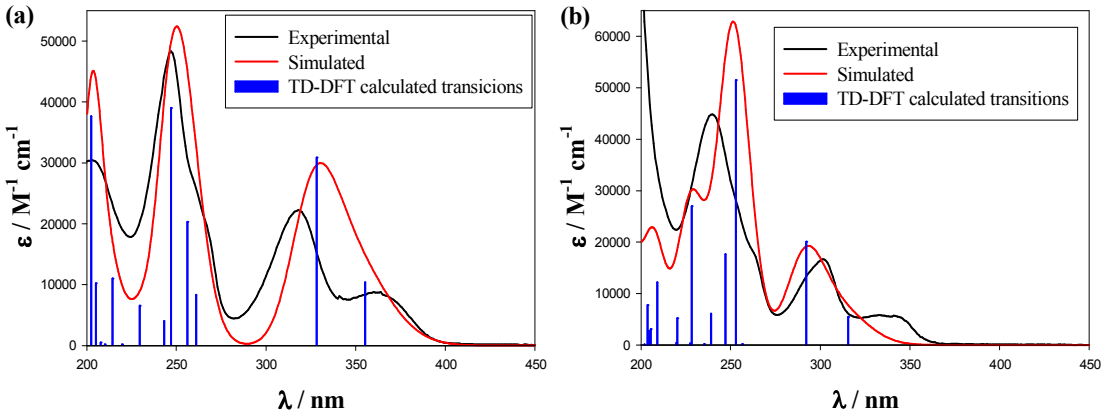

Figure 4: Comparison of the UV-vis experimental absorption spectrum (black lines) with TD-DFT calculated electronic transitions (blue lines) and simulated spectra (red lines) for **(a)** 6-Cl-HaH$^+$ and **(b)** 6-Cl-Ha. The vertical transition energies were calculated at the optimized ground-state geometry by TD-DFT calculations (see text for details).

Steady-state and time-resolved fluorescence emission

Fluorescence measurements were recorded in both acidic and alkaline aqueous solutions (Figure 5). Briefly, under acidic conditions (pH 4.0), a single emitting species was observed for the three chloroharmines investigated. Emission spectra showed one intense-broad band (centred at ~430 nm) and time-resolved analysis yields mono-exponential decays over the entire emission range (with lifetimes ~2 ns). The latter emitting species were assigned to protonated or cationic (C) chloroharmines. On the other hand, fluorescence spectra recorded under alkaline conditions (pH 9.0) showed two additional pH-dependent emission bands centred at ~380 nm and ~470 nm (shoulder), besides the emission band at ~430 nm. Fluorescence decays recorded at each maximum wavelength of emission (treated as bi-exponential) showed the presence of three distinctive emission-wavelength-dependent species, with lifetimes of ~0.5 ns, ~2 ns and ~8 ns. According to the information reported for other related βCs and data recorded under acidic conditions, the three emitting species were assigned to neutral (N), protonated or cationic (C) and zwitterionic (Z)[65] species of βCs, respectively.

Both protonated and neutral species show a noticeable shift of the maximum of emission relative to Ha of ~ +15 nm. This is consistent with the bathochromic shift observed on the UV-vis absorption spectra (*vide supra*). Besides, the presence of zwitterionic species upon excitation of alkaline (pH ≤ 9.0) chloroharmines represents another distinctive behaviour with respect to Ha. Note that, although the presence of Ha-zwitterion species in alkaline (pH > 11) organic-protic solvents has been reported in the literature, it was not detected under our experimental conditions (*i.e.*, moderate-alkaline aqueous solution). This is further supported by time-resolved fluorescence data (*vide infra*).

View Article Online
DOI: 10.1039/C5CP05866J

The presence of the emission band at ~430 nm evidences that photoexcited chloroharmines show the typical enhancement of the basicity of the βC pyridinic nitrogen.[36] When the electronic excited state becomes populated, even in water at pH 9.0, a fraction of the excited neutral species is protonated during the lifetime of its S_1 state. However, in contrast to what was observed for Ha and other βCs,[27, 35, 36] the relative intensity of both emitting bands of chloroharmines is quite similar (Figure 5b) suggesting that only a fraction (≤ 50%) of neutral excited chloroharmines follows protonation to yield the corresponding protonated excited chloroharmine cation, which then emits.

It is also important to note that the intensity of fluorescence observed upon excitation of the three compounds studied is significantly lower than that of Ha, showing a considerable difference in Φ_F (Table 1). This suggests that chlorine atoms, attached to the βC moiety, enhance other deactivation pathways different than fluorescence emission. It is well known that heavy atoms attached directly to aromatic compounds can reduce significantly the Φ_F (because of the so called intramolecular heavy atom effect).[66, 67] Typically, the spin-orbital coupling mechanism of the heavy atom enhances the rate of intersystem crossing to the triplet state ($S_1 \rightarrow T_1$). However, our singlet oxygen data independently obtained as well as the data on chloroharmines photodegradation (*vide infra*) suggest that internal conversion ($S_1 \rightarrow S_0$) might be the operative deactivation pathway.

The corresponding quantum yields of fluorescence (Φ_F) and other selected photophysical properties are collected in Table 1. Chloroharmines show the same trend to that observed for other βCs: neutral species have Φ_F values rather smaller than the corresponding protonated species. In the case of 6-Cl-Ha, it was also demonstrated that the data obtained are consistent with the corresponding low values of quantum yield of 6-Cl-Ha consumption (Φ_R) observed. To the best of our knowledge, emission spectra and Φ_F values of both acid-base species of chloroharmine dissolved in aqueous solution have not previously been reported.

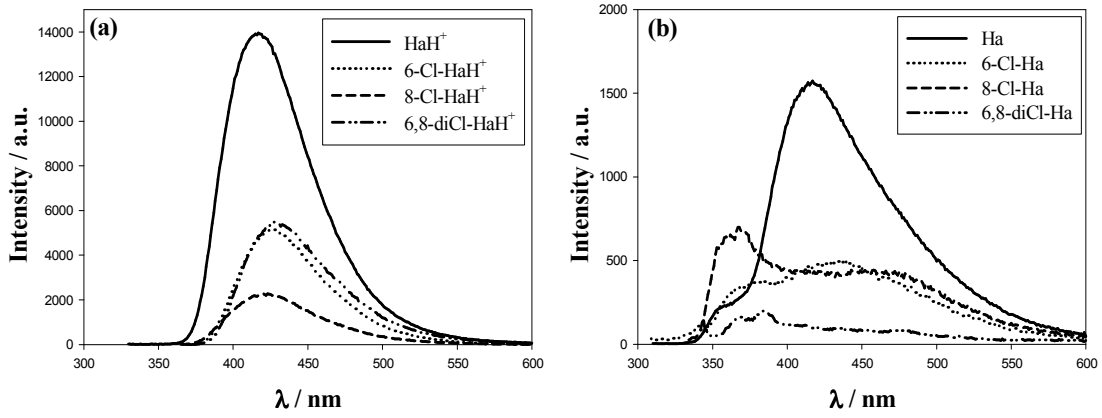

Figure 5. Fluorescence emission spectra of chloroharmine derivatives recorded in: **(a)** acidic (pH 4) and **(b)** alkaline (pH 9.0) aqueous solutions.

View Article Online
DOI: 10.1039/C5CP05866J

On the contrary to what had been previously described for other protonated βC derivatives, the typical oxygen-concentration-dependent decrease in Φ_F was not observed in the case of the three chloroharmines studied. The data clearly showed that Φ_F was independent, within the experimental error, on the increase of oxygen partial pressure (Table 1, entries 9-11). This fact could be the consequence of the relatively short fluorescence lifetime of protonated chloroharmine derivatives (~2 ns, see Table 1) compared with other βCsH^+ described (~20 ns).[36, 37]

Laser flash photolysis

Due to the extremely low solubility of chloroharmines in alkaline aqueous media, laser flash photolysis experiments were performed exclusively with the protonated species (acidic conditions). According to the literature, the excitation of oxygen-free solutions of related βCs (such as norharmane, harmane, harmine, among others) generates a transient species that absorbs throughout the visible spectrum with triplet-lifetimes ranging from 30 μs to 5 ms, depending on the pH and the solvent used.[37, 68-70] In aqueous solutions, the transient absorption spectra of protonated βCs (pH < 5) show two bands at ~450 and 580 nm, whereas the spectra of neutral species (pH > 9) has only one band centred at ~510 nm. Thus, for protonated-chloroharmines 450 nm was the wavelength used to monitor and record the kinetic traces obtained in a time-resolved triplet state absorption experiment (see kinetic traces in Figures 6 and ESI.7).

Oxygen-free solutions of chloroharmines, when subject to laser-pulse excitation, generate two transient species (Table 1, entry 18). On the basis of previous reports, the short-lived transient was assigned to the triplet (T_1) state; whereas the long-lived transient might originate from the chloroharmine photo-degradation. It is noteworthy that the traces do not reach the baseline, as expected for an irreversible photochemical transformation. Moreover, UV-vis absorption spectra of irradiated solutions showed noticeable changes, indicative for the presence of an irreversible photochemical reaction (*vide infra*).

In the presence of oxygen (*i.e.*, in aerated and O_2-saturated solutions), all the kinetic traces show mono-exponential decay, where only the short-live transient (with lifetimes ~1.5 μs and ~0.25 μs, in air-equilibrated and O_2-saturated solutions, respectively) can be observed, corresponding to T_1.[71] For all three compounds in acidic water, the fast transient was quenched by O_2 with a rate constant of $\sim 2.5 \times 10^9$ M^{-1} s^{-1} (Table 1, entry 21).

View Article Online
DOI: 10.1039/C5CP05866J

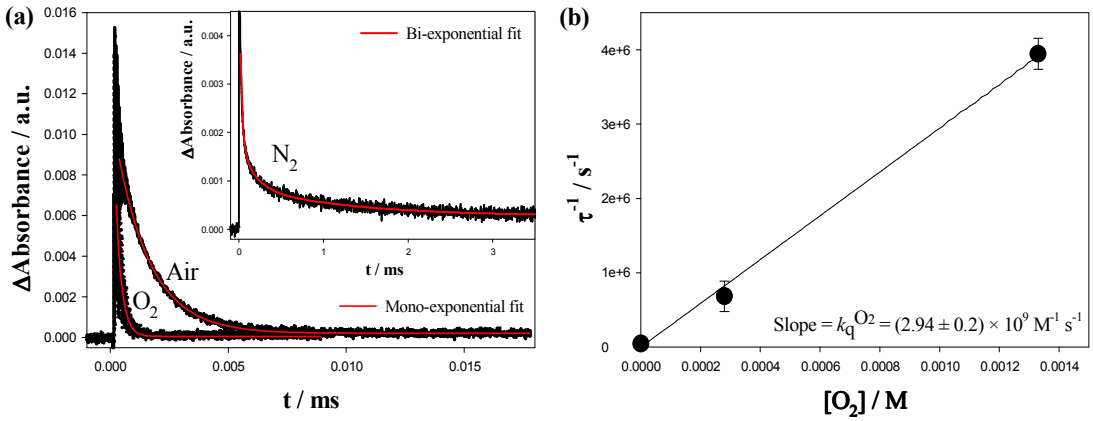

Figure 6. (a) Kinetic traces obtained in a time-resolved triplet state absorption experiment of 6-Cl-HaH$^+$, dissolved in H_2O at pH 4. Data are shown for N_2-saturated (*inset*), air-equilibrated and O_2-saturated solutions. Superimposed on the data are double and single exponential fitting functions used in the analysis of experiments run in absence and presence of oxygen, respectively. **(b)** Plot of the first-order rate constant for the decay of the triplet state against the dissolved oxygen concentration.

Table 1: Photochemical and photophysical parameters determined upon one-photon excitation of chloroharmine derivatives in aqueous solution under acidic and alkaline conditions (pH 4.0 and 9.0, respectively). Data for harmine are listed for comparative porpoise.

Entry		6-Cl-Ha		8-Cl-Ha		6,8-diCl-Ha		Ha	
	Acid-base species	Protonated	Neutral	Protonated	Neutral	Protonated	Neutral	Protonated	Neutral
1	**pK_{a1}**	6.3 ± 0.2		6.4 ± 0.2		5.4 ± 0.4		7.5, [a] 8.0 or [b] 7.7	
2	**pK_{a2}**	10.5 ± 0.3		nd		nd		[a] 14.5 or [b] > 14	
3	**λ_{obs}^{Abs} / nm**	362 ($S_0 \rightarrow S_1$) 317 ($S_0 \rightarrow S_2$)	342 ($S_0 \rightarrow S_1$) 302 ($S_0 \rightarrow S_2$)	361$^{(sh)}$ ($S_0 \rightarrow S_1$) 321 ($S_0 \rightarrow S_2$)	340 ($S_0 \rightarrow S_1$) 298 ($S_0 \rightarrow S_2$)	369 ($S_0 \rightarrow S_1$) 305 ($S_0 \rightarrow S_2$)	357 ($S_0 \rightarrow S_1$) 293 ($S_0 \rightarrow S_2$)	357$^{(sh)}$ ($S_0 \rightarrow S_1$) 320 ($S_0 \rightarrow S_2$)	332 ($S_0 \rightarrow S_1$) 298 ($S_0 \rightarrow S_2$)
4	[c] **λ_{calc}^{Abs} / nm**	355.26 ($S_0 \rightarrow S_1$) 328.20 ($S_0 \rightarrow S_2$)	315.61 ($S_0 \rightarrow S_1$) 229.19 ($S_0 \rightarrow S_2$)	345.70 ($S_0 \rightarrow S_1$) 336.40 ($S_0 \rightarrow S_2$)	313.30 ($S_0 \rightarrow S_1$) 290.50 ($S_0 \rightarrow S_2$)	362.00 ($S_0 \rightarrow S_1$) 329.70 ($S_0 \rightarrow S_2$)	325.80 ($S_0 \rightarrow S_1$) 281.90 ($S_0 \rightarrow S_2$)	nd	
5	**$\varepsilon_{obs} \times 10^{-4}$ / M^{-1} cm^{-1}**	0.902 ($S_0 \rightarrow S_1$) 2.406 ($S_0 \rightarrow S_2$)	0.566 ($S_0 \rightarrow S_1$) 1.666 ($S_0 \rightarrow S_2$)	0.588 ($S_0 \rightarrow S_1$) 1.672 ($S_0 \rightarrow S_2$)	0.414 ($S_0 \rightarrow S_1$) 1.603 ($S_0 \rightarrow S_2$)	0.633 ($S_0 \rightarrow S_1$) 1.890 ($S_0 \rightarrow S_2$)	0.558 ($S_0 \rightarrow S_1$) 0.871 ($S_0 \rightarrow S_2$)	0.734 ($S_0 \rightarrow S_1$) 1.757 ($S_0 \rightarrow S_2$)	0.371 ($S_0 \rightarrow S_1$) 1.102 ($S_0 \rightarrow S_2$)
6	[c] **$f_{osc\ calc}$**	0.1300 ($S_0 \rightarrow S_1$) 0.3857 ($S_0 \rightarrow S_2$)	0.0697 ($S_0 \rightarrow S_1$) 0.2558 ($S_0 \rightarrow S_2$)	0.0605 ($S_0 \rightarrow S_1$) 0.4407 ($S_0 \rightarrow S_2$)	0.0752 ($S_0 \rightarrow S_1$) 0.2847 ($S_0 \rightarrow S_2$)	0.0795 ($S_0 \rightarrow S_1$) 0.3839 ($S_0 \rightarrow S_2$)	0.0772 ($S_0 \rightarrow S_1$) 0.1343 ($S_0 \rightarrow S_2$)	--	--
7	**Major contributions to Electronic Transitions (% coefficients)**	H→L (81%), H–1→L (15%) ($S_0 \rightarrow S_1$) H–1→L (81%), H→L (13%) ($S_0 \rightarrow S_2$)	H→L (93%) ($S_0 \rightarrow S_1$) H–1→L (86%), H→L+1 (11%) ($S_0 \rightarrow S_2$)	H–1→L (80%), H→L (17%) ($S_0 \rightarrow S_1$) H→L (79%), H–1→L (15%) ($S_0 \rightarrow S_2$)	H→L (85%) ($S_0 \rightarrow S_1$) H–1→L (76%), H→L+1 (11%) ($S_0 \rightarrow S_2$)	H→L (96%) ($S_0 \rightarrow S_1$) H–1→L (94%) ($S_0 \rightarrow S_2$)	H→L (95%) ($S_0 \rightarrow S_1$) H–1→L (72%) ($S_0 \rightarrow S_2$)	--	--
9	[d] **Φ_R (air)**	7.8×10^{-3}	3.2×10^{-3}	5.7×10^{-3}	nd	4.8×10^{-3}	nd	3.7×10^{-3}	1.63×10^{-3}
10	[d] **Φ_{H2O2} (air)**	1.79×10^{-3}	0.76×10^{-3}	0.77×10^{-3}	nd	1.9×10^{-3}	nd	0.84×10^{-3}	0.37×10^{-3}
11	**λ_{max}^{fluo} / nm**	428 ± 1 (C)	375 ± 1 (N) 426 ± 1 (C) 467 ± 5 (Z)	423 ± 2 (C)	356 ± 2 (N) 423 ± 5 (C) 460 ± 3 (Z)	429 ± 1 (C)	361 ± 2 (N) 429 ± 5 (C) 475 ± 3 (Z)	[e] 416 ± 2 (C)	[e] 358 ± 1 (N) [e] 415 ± 1 (C)
12	**Φ_F (N_2)**	0.16 ± 0.01	0.12 ± 0.03	0.11 ± 0.02	0.11 ± 0.01	0.20 ± 0.02	0.017±0.001	0.47 ± 0.05	0.39 ± 0.05
13	**Φ_F (air)**	0.16 ± 0.02	0.12 ± 0.05	0.11 ± 0.02	0.12 ± 0.01	0.20 ± 0.02	0.017±0.001	0.49 ± 0.05	0.38 ± 0.05
14	**Φ_F (O_2)**	0.16 ± 0.02	0.10 ± 0.04	0.11 ± 0.02	0.10 ± 0.01	0.20 ± 0.02	0.017±0.001	0.47 ± 0.05	0.36 ± 0.05
15	[f] **τ_F / ns**	2.2(at 426 nm, C)	0.4 (at 375 nm, N) 2.1 (at 426 nm, C) 8.5-12 (at 510 nm, Z)	2.23(at 423 nm, C)	0.59 (at 360 nm, N) 2.32 (at 423 nm, C) 8.59 (at 480 nm, Z)	2.80 (at 429 nm, C)	0.22 (at 370 nm, N) 2.20 (at 430 nm, C) 7.50 (at 485 nm, Z)	7.06 (at 416 nm, C)	0.44 (at 358 nm, N) and 6.96 (at 415 nm, C)
16	**λ_{em}^{phos} / nm**	[g] 472	[g] 473	[g] 481	[g] 476	[g] 473	[g] 434	[i] 437, [h] 460	[i] 396, [h] 405
17	**E_T / kJ mol^{-1}**	253.5	252.9	248.7	251.3	252.9	275.6	[i] 274.4, [h] 265.8	[i] 302.1, [h] 295.4
18	[j] **τ_T / µs (N_2)**	22 [k] (and 150)	nd	48 [k] (and 80)	nd	11 [k] (and 48)	nd	27 and 160, [i] 530	--
19	[j] **τ_T / µs (air)**	1.5	nd	1.5	nd	1.7	nd	1.6, [i] --	--
20	[j] **τ_T / µs (O_2)**	0.25	nd	0.28	nd	0.31	nd	0.25, [i] --	--
21	[j] **k_q^{O2}/ M^{-1} s^{-1}**	2.94×10^9	nd	2.49×10^9	nd	2.41×10^9	nd	2.97×10^9	nd
22	**Φ_Δ (air, in D_2O)**	0.19 ± 0.03	nd	0.22 ± 0.04	nd	0.05 ± 0.02	nd	[e] 0.22 ± 0.02	[e] 0.13 ± 0.01
23	**Φ_Δ (O_2, in D_2O)**	0.19 ± 0.03	nd	0.26 ± 0.04	nd	0.08 ± 0.02	nd	[e] 0.24 ± 0.02	[e] 0.13 ± 0.01
24	[l] **k_t^Δ (in D_2O) / M^{-1} s^{-1}**	1.4×10^7	nd	4.3×10^7	nd	1.6×10^7	nd	3.6×10^6	3.5×10^7

nd = non-determined data due to the extremely low solubility and/or due to the thermal decomposition of alkaline solutions of the investigated compounds in the course of the experiment. sh = the band appears as a shoulder of the $S_1 \rightarrow S_0$ transition. [a] Data obtained from Ref. [60]. [b] Data obtained from Ref. [72]. [c] Method: TD-DFT calculations (see text for details). [d] Error of ± 0.3 on the mantissa shown. [e] Data obtained from Ref. [36]. [f] Decays recorded under acidic and alkaline conditions were mono- and bi-exponential, respectively. [g] Method: phosphorescence emission at low-temperature. Note that λ_{em}^{phos} values reported in Ref. [31] are inaccurate [h] Data obtained from Ref. [31]. [i] Data obtained from Ref. [68]. Method: measured in N_2-saturated acidic (pH 0) aqueous media by microsecond flash photolysis. [j] Method: laser flash photolysis. [k] Lifetime shown in parenthesis is assigned to a transient species that lead to the degradation product. [l] k_t^Δ is the rate constant of total quenching of $^1O_2$ by βC.

View Article Online
DOI: 10.1039/C5CP05866J

Stability of chloroharmine upon UVA steady-state excitation

Air-equilibrated chloroharmine aqueous solutions were irradiated and reactions were monitored by UV-visible spectrophotometry and HPLC. Figure 7 shows, as a representative example, data obtained for 6-Cl-HaH$^+$. Briefly, significant changes in the absorption spectrum were observed during UVA irradiation (Figure 7a). The decrease in the βC concentration, as a function of elapsed irradiation time, follows zero-order kinetics during the first 30 min of irradiation (Figure 8a and ESI.8). The three investigated chloroharmine showed quite small quantum yields values for the βC disappearance, Φ_R, (Table 1, entry 9). Moreover, for those compounds that showed thermal stability under alkaline conditions (6-Cl-Ha and Ha)[73], the expected dependence of Φ_R on pH was observed, with the neutral species being more stable than the protonated ones.[35, 36] When comparing the observed Φ_R values, it is evident that the presence of the chlorine atom makes 6-Cl-Ha less photo-stable than Ha (*vide infra*).

Experiments performed under anaerobic conditions (*i.e.*, N_2-saturated) were used to further explore the role of dissolved molecular oxygen in the photochemical pathway/s of 6-Cl-HaH$^+$ consumption, as well as the presence of radical reactions. In contrast to what was observed for other βCs[35, 36], 6-Cl-HaH$^+$ showed to be unstable upon UVA excitation (Figure 7b), even in anaerobic conditions, with a Φ_R value of 7.9×10^{-3}. The latter value was the same, within the experimental error, to that observed in the presence of oxygen. Nevertheless, photoinduced spectral changes indicate that the pattern of the studied reaction strongly depends on the dissolved-oxygen concentration (see comparative NED spectra in Figure 7c). The reactions in absence and presence of oxygen follow a quite different pattern, suggesting the presence of at least two distinctive types of reactions (*vide infra*).

When subject to UVA-irradiation, carbon-chlorine bonds usually follow homolytic-cleavage yielding Cl$^\bullet$ and βC$^\bullet$. In aqueous environment, Cl$^\bullet$ can take a hydrogen atom either from the solvent (water) or from organic molecules (6-Cl-HaH$^+$) yielding, as consequence, H^+ and Cl^- (reactions 5 and 7). To further explore this, we measured herein the evolution of chloride ion and proton concentrations during the irradiation of both anaerobic and aerobic 6-Cl-HaH$^+$ solutions. For these experiments, the initial pH of the solution was adjusted by adding drops of $HClO_4$, in order to minimize the initial concentration of chloride in the solution. The profile and the rate of the photochemical reactions were independent of the inorganic acid used (see Figure ESI.9). In the studied example, chloride ions and protons are released while 6-Cl-HaH$^+$ is being irradiated (see entries 1 and 2 in Table 2 and Figure 8b). These results are consistent with the decrease in the calculated electron density distributions on chlorine atoms described for excited states (*vide supra*).

View Article Online
DOI: 10.1039/C5CP05866J

Note that: ***(i)*** Under both anaerobic and aerobic conditions about one chloride ion and two protons are released per each molecule of 6-Cl-HaH$^+$ consumed (see entry 2 in Table 2 and Figure 8b). ***(ii)*** Φ_{Cl^-} observed in argon is slightly higher than that observed in the presence of oxygen, suggesting the presence of an additional deactivation process competing by the photo-excited chloroharmine. ***(iii)*** Curves of proton release as a function of irradiation time show a stationary-phase-like pattern (being more evident in anaerobic experiments). This fact suggests that protons are produced in a secondary reaction. ***(iv)*** Harmine was not detected as a photoproduct neither in anaerobic nor in aerobic conditions, suggesting that Ha$^\bullet$ produced upon C-Cl cleavage in 6-Cl-Ha would not react with the solvent (via hydrogen abstraction) to yield Ha. Reaction 9 might represent a possible fate of this radical.

Results shown above are consistent with the reasonable expectation that, although the photo-initiated degradation of chloro-βCs depends on the presence of oxygen (reaction 12) (*vide infra*), a parallel and competitive radical-pathway might also play a key role in the mechanism of reaction: *i.e.*, through homolytic-cleavage of C-Cl bonds (reaction 4). These results are in agreement with laser flash photolysis results (*vide supra*).

View Article Online
DOI: 10.1039/C5CP05866J

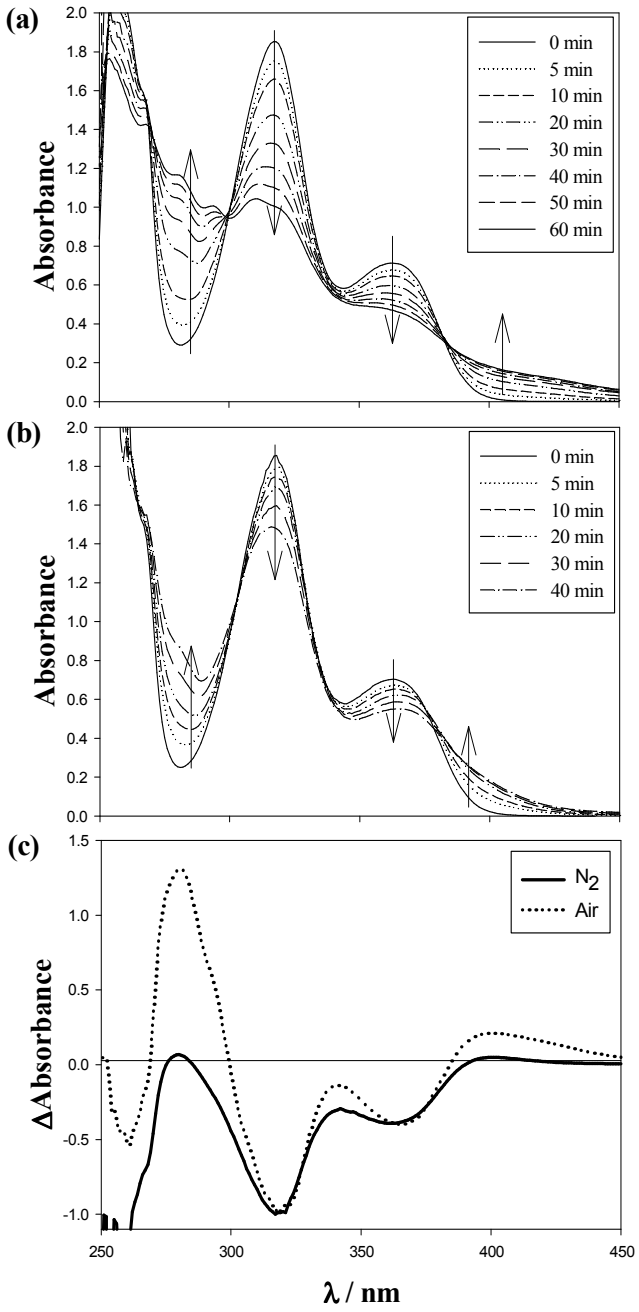

Figure 7. Evolution of the UV-vis spectra of air-equilibrated **(a)** and N_2-saturated **(b)** 6-Cl-HaH$^+$ ($[\beta C]_0$ = 80 µM, pH 4.0) aqueous solutions as a function of irradiation time. **(c)** Normalized (at 317 nm) Experimental Difference (NED) spectra.

Hydrogen peroxide (H_2O_2) production under UVA steady-state irradiation

The production of H_2O_2 was detected upon irradiation of air-equilibrated solutions of chloroharmines (Figure 8a and Figure ESI.8). Filled (black) symbols in Figure 8a represent the evolution of the concentration of H_2O_2 as a function of elapsed irradiation time ($[\beta C]_0$ = 150 µM, pH 4.0), whereas open symbols represents the evolution of the βCs' concentration. Quantum yields

View Article Online
DOI: 10.1039/C5CP05866J

of H_2O_2 formation ($\Phi_{H_2O_2}$) listed in Table 1 (entry 10) show that although photoexcited chloroharmines have a very low efficiency of H_2O_2 production, $\Phi_{H_2O_2}$ depends noticeably on the position of the chlorine atom (being the 6-substituted derivatives 6-Cl-Ha and 6,8-diCl-Ha more efficient than 8-Cl-Ha) and also on the pH (being the neutral form less efficient than the protonated form).

The production of H_2O_2 upon UVA irradiation of βCs has been reported.[35, 36] In an earlier study of norharmane,[35] it was suggested that H_2O_2 is formed by electron transfer from S_1 to O_2 yielding the superoxide anion ($O_2^{\bullet-}$) and, as a result of the spontaneous disproportionation of $O_2^{\bullet-}$, H_2O_2 is produced. This may indeed be one source of H_2O_2 that is applicable in our present work (reaction 14). This hypothesis is further supported by the increase in the $\Phi_{H_2O_2}$ value observed when experiments were performed in the presence of SOD enzyme (Table 2, entry 4).

H_2O_2 might be also produced in the anaerobic pathway (*vide supra*) as a consequence of $HO^{\bullet}$ self-annihilation (reaction 10). As it was expected, the latter hypothesis was confirmed by measuring the production of H_2O_2 in irradiated argon-saturated 6-Cl-HaH^+ solutions. In particular, a $\Phi_{H_2O_2}$ value of 1.0×10^{-3} was determined (Table 2, entry 1).

$\Phi_{H_2O_2}$ and Φ_R values (Table 2) are the same order of magnitude suggesting that H_2O_2 (or compounds related to its formation, *i.e.*, $O_2^{\bullet-}$) may be involved, at least in part, in the photo-initiated degradation of chloroharmines. Comparison of Φ values listed in Table 2 shows a ratio between 6-Cl-HaH^+ consumed and H_2O_2 produced of ~ 4 to 1 (*i.e.*, far from the 2 to 1 ration expected from the reactions described in the previous paragraph). The latter fact suggests the presence of additional reactive pathways of $O_2^{\bullet-}$ and/or $HO^{\bullet}$ consumption, that might be reactions 8, 9 and 15.

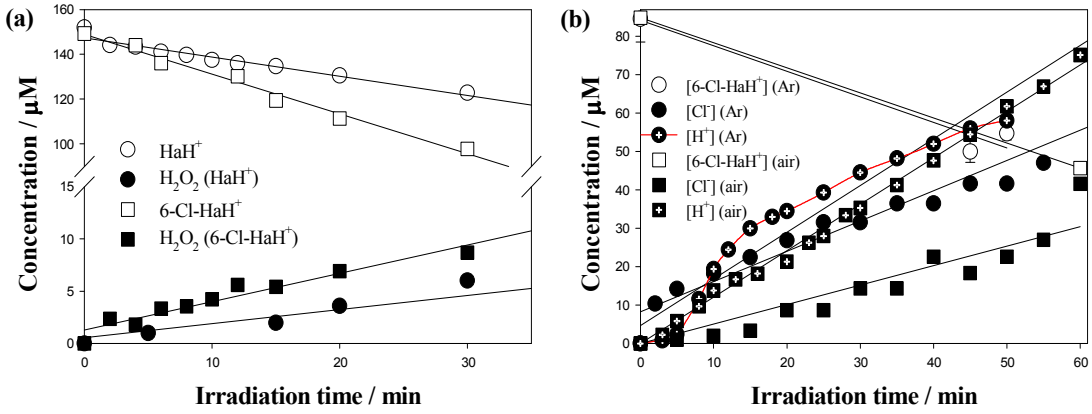

Figure 8. (a) Evolution of βC and H_2O_2 concentration in air-equilibrated aqueous solutions of HaH^+ (circles) and 6-Cl-HaH^+ (squares) as a function of irradiation time ($[\beta C]_0$ = 150 μM, pH 4.0). **(b)** Evolution of 6-Cl-HaH^+ and chloride (Cl^-) concentration in Ar-saturated (circles) and air-equilibrated aqueous solutions (squares) as a function of irradiation time ([6-Cl-HaH^+] = 85 μM, pH 4.0).

Quantum yield of chloroharmines sensitized $^1O_2$ production (Φ_Δ) in aqueous solution

View Article Online
DOI: 10.1039/C5CP05866J

It has been proposed that βC alkaloids are excellent $^1O_2$ photosensitizers.[74] Values of Φ_Δ for the neutral form of norharmane, harmane and harmine in aprotic organic solvents were found to be ranged from 0.31 to 0.40.[69] However, we have recently demonstrated that, in aqueous environment βCs show quite small Φ_Δ values (ranged from 0.06 to 0.24, depending on the βCs, the pH and also on the dissolved oxygen concentration).[27, 35, 36] Briefly, for a given βC derivative, the higher the pH, the lower the Φ_Δ; whereas the higher the $[O_2]$, the higher the Φ_Δ.

We have determined herein the quantum yields for the photosensitized production of $^1O_2$ and the rate constant of total quenching of $^1O_2$ (k_t^Δ) by the three chloroharmines studied in acidic aqueous solution (alkaline solutions were unstable over the time interval of the measurements). The data, recorded as a function of ambient oxygen partial pressure (*i.e.*, exposure to air and oxygen), are listed in Table 1. Regarding this, some key points might be highlighted: *(i)* the efficiency of $^1O_2$ production depends on the chemical structure of the βC derivative ($\Phi_\Delta^{6\text{-Cl-Ha}} \approx \Phi_\Delta^{8\text{-Cl-Ha}} >> \Phi_\Delta^{6,8\text{-diCl-Ha}}$). *(ii)* Within the experimental error, no change was observed in Φ_Δ of all investigated compounds with the increase in the oxygen concentration ($\Phi_\Delta^{(O_2)} \approx \Phi_\Delta^{(air)}$). This is in good connection with the oxygen-induced triplet state deactivation described above. Triplet-triplet energy transfer might be the operative pathway for $^1O_2$ production. *(iii)* In the cases of 6-Cl-Ha and 8-Cl-Ha, the Φ_Δ values listed in Table 1 ($\Phi_\Delta^{(air)}$ = 0.19 and 0.22, respectively) are quite similar to the corresponding value reported for Ha ($\Phi_\Delta^{(air)}$ = 0.22). Thus, no heavy-atom effect was observed due to the presence of chlorine atoms. *(iv)* Φ_Δ values obtained are entirely consistent with Φ_F values recorded at the same oxygen concentration in independent experiments (the sum of Φ_Δ and Φ_F does not exceed 1.0). *(v)* On the contrary to what was described for other βCs, as an exception to the rule,[36, 37] the lack of a dependence of Φ_F values on the dissolved oxygen concentration and the quite high Φ_Δ values observed for chloroharmines (~0.2) suggest that triplet-triplet energy transfer might be the operative pathway for $^1O_2$ production reported herein. *(vi)* k_t^Δ values observed for protonated chloroharmines were about one order of magnitude higher than that observed for the unsubstituted Ha (Table 1, entry 24). Although k_t^Δ values for neutral chloroharmines could not be measured, a predictive modelling of the total deactivation rate constant of singlet oxygen by heterocyclic compounds suggest that neutral βCs would have k_t^Δ values one order of magnitude higher than protonated βCs (*i.e.*, ~10^8 and ~10^7, respectively).[75]

Role of reactive oxygen species (ROS) in the photochemistry of 6-chloroharmine

The contribution of ROS produced by photoexcited 6-Cl-HaH$^+$ (*vide supra*) to its photo-degradation was investigated in four independent experiments. Briefly, quantum yields of 6-Cl-

View Article Online
DOI: 10.1039/C5CP05866J

HaH^+ consumption (Φ_R) were determined in the presence of propan-2-ol, SOD, catalase and sodium azide, to evaluate the role of $HO^\bullet$, $O_2^{\bullet-}$, H_2O_2 and $^1O_2$, respectively (Figure ESI.10a).[35] Results, listed in Table 2, show that catalase has no significant effect on the efficiency of 6-Cl-HaH^+ consumption, whereas propan-2-ol, SOD and NaN_3 induce a small decrease (~ 5 - 25%) on the Φ_R with respect to the experiment performed in the absence of these scavengers. Thus, $Cl^\bullet$, $HO^\bullet$, $O_2^{\bullet-}$ and/or $^1O_2$ might play a secondary role in the main mechanism of 6-Cl-HaH^+ photodegradation (*i.e.*, reactions 5, 8, 15 and 16).

The quantum yields of H_2O_2 production (Φ_{H2O2}) were also measured in the presence of ROS scavengers in order to investigate which ROS ($HO^\bullet$, $^1O_2$ and/or $O_2^{\bullet-}$) promotes the production of H_2O_2 described above (Figure ESI.10b). Results, obtained in the presence of propan-2-ol, suggest that $HO^\bullet$ is not the precursor of H_2O_2 produced (Table 2, entry 3). On the other hand, although $^1O_2$ might have a minor contribution through endoperoxide intermediates (Table 2, entry 5), the quite high increase on the Φ_{H2O2} observed in the presence of SOD clearly indicates that $O_2^{\bullet-}$ is the main H_2O_2 precursor; chloroharmines follow the same trend to that described for other βCs.[35, 36]

Table 2: Quantum yields of 6-Cl-HaH^+ consumption (Φ_R) and H_2O_2 production (Φ_{H2O2}) upon UVA (350 nm) excitation of 6-Cl-HaH^+ acidic aqueous solutions (pH 4.0) in absence and in presence of different reactive oxygen species (ROS) scavengers.

Entry	Experimental condition	[a] Φ_R	[a] Φ_{H2O2}	[a] Φ_{H+}	[a] Φ_{Cl-}
1	**Φ_R (argon)**	7.9×10^{-3}	1.0×10^{-3}	14.5×10^{-3}	9.4×10^{-3}
2	**Φ_R (air)**	7.8×10^{-3}	1.8×10^{-3}	14.4×10^{-3}	6.1×10^{-3}
3	**[a] Φ_R (air, + propan-2-ol)**	7.2×10^{-3}	1.7×10^{-3}	--	--
4	**[a] Φ_R (air, + SOD)**	6.4×10^{-3}	6.8×10^{-3}	--	--
5	**[a] Φ_R (air, + NaN_3)**	6.4×10^{-3}	3.1×10^{-3}	--	--
6	**[a] Φ_R (air, + catalase)**	7.6×10^{-3}	0.2×10^{-3}	--	--

[a] Error of ± 0.3 on the mantissa shown.

Proposed mechanism of reactions

According to the results above described the following reaction scheme is proposed for the first steps of the photochemical reaction of 6-Cl-HaH^+ (a representative example of chloroharmines) in aqueous solution, at pH 4.0:

Reaction

$$6\text{-Cl-HaH}^+ \xrightarrow{h\nu} [^1\text{6-Cl-HaH}^+]^* \quad (1)$$

O_2-independent pathway:

$$[^1\text{6-Cl-HaH}^+]^* \longrightarrow \text{6-Cl-HaH}^+ + h\nu' \text{ (428 nm)} \quad (2)$$

$$[^1\text{6-Cl-HaH}^+]^* \xrightarrow{\text{ISC}} [^3\text{6-Cl-HaH}^+]^* \quad (3)$$

View Article Online
DOI: 10.1039/C5CP05866J

$[^3$6-Cl-HaH$^+]^*$ → $[HaH^+]^{\cdot} + Cl^{\cdot}$ (4)

6-Cl-HaH$^+ + Cl^{\cdot}$ → 6-Cl-Ha(-H)H$^{\cdot+} + Cl^- + H^+$ (5)

$Cl^{\cdot} + Cl^{\cdot}$ → Cl_2 (6)

$Cl^{\cdot} + H_2O$ → $Cl^- + H^+ + HO^{\cdot}$ (7)

$HO^{\cdot}$ + 6-Cl-HaH$^+$ → 6-Cl-Ha(-H)H$^{\cdot+} + H_2O$ (8)

$HO^{\cdot} + [HaH^+]^{\cdot}$ → HO-HaH$^+$ (9)

$HO^{\cdot} + HO^{\cdot}$ → H_2O_2 (10)

Other radical species, such as $Cl_2^{\cdot-}$, might be formed and, consequently, additional reactions would then contribute to the total 6-Cl-HaH$^+$ consumption. Additional experiments are needed to further investigate this hypothesis.

O_2-dependent pathway:

$[^3$6-Cl-HaH$^+]^*$ + $^3O_2$ $\xrightarrow{k_{ET}}$ 6-Cl-HaH$^+$ + $^1O_2$ (11)

$[^1$6-Cl-HaH$^+]^*$ + $^3O_2$ $\underset{k'_{et}}{\overset{k_{et}}{\rightleftharpoons}}$ $[6\text{-Cl-Ha}]^{\cdot+}$ + $HO_2^{\cdot}$ (12)

$HO_2^{\cdot}$ $\overset{pK_a = 4.8}{\rightleftharpoons}$ $O_2^{\cdot-} + H^+$ (13)

$O_2^{\cdot-} + HO_2^{\cdot} + H^+$ → $H_2O_2 + O_2$ (14)

6-Cl-HaH$^+ + HO_2^{\cdot}$ $\xrightarrow{k_t}$ 6-Cl-Ha(-H)H$^{\cdot+} + H_2O_2$ (15)

6-Cl-HaH$^+ + {}^1O_2$ $\xrightarrow{k_t}$ physical and chemical $^1O_2$ deactivation (16)

Based on the reaction of other related βCs, the radicals $[6\text{-Cl-Ha}]^{\cdot+}$ and 6-Cl-Ha(-H)H$^{\cdot+}$ would follow two competitive dimerization pathways previously described for norharmane, harmane and harmine in dichloromethane solution[76]: *(i)* the reaction with another molecule of 6-Cl-HaH$^+$ in its ground state and/or *(ii)* the anhilation with another radical $[6\text{-Cl-Ha}]^{\cdot+}$. In this regards, $[HaH^+]^{\cdot}$ might follow similar processes.

CONCLUSIONS

Data presented herein make this study relevant from the biological point of view. These particular approaches represent basic research that provides, at a molecular level, relevant information that can be a stepping stone on the way of understanding the biological role of these alkaloids and/or to suggest possible biological functions: *(i)* due to the quite low efficiency showed by these compounds to photoinduce ROS formation, instead of being photo-triggered active compounds against invasive microorganism via ROS (as it has been suggested)[77], they can act in ROS-mediated intracellular signalling. *(ii)* The quite high k_t^{Δ} values observed (~ 10^7 - 10^8) make halogenated βCs good candidates to act as antioxidant in living systems, under photoinduced oxidative stress. *(iii)* Chloro-βC alkaloids found in nature, such as Bauerine, has a methyl group

View Article Online
DOI: 10.1039/C5CP05866J

bound to the pyrrolic nitrogen (N-9).[11] Having in mind that under physiological pH conditions the neutral species of chloro-βCs are present in more than 50 - 70% (*vide supra*), such a methylation might act as a protective response to thermal hydrolysis showed by neutral non-methylated-chloroharmines, where the hydrogen atom at N-9 seems to play a key role in the mentioned reaction. Certainly, this hypothesis should be further considered.

On the other hand, this study will also provide the chance to further explore other fundamental aspects. As an example, in the search of a better photosensitizer (more effective, at a low dose, absorbing in the far UVA and/or visible region) the herein investigated chloroharmines showed quite distinctive photophysical and photochemical properties that make them good candidates that deserve to be further inspected from this point of view.

Electronic supplementary information (ESI) available: Spectrophotometric titration of 6-chloroharmine (6-Cl-Ha), 8-chloroharmine (8-Cl-Ha) and 6,8-dichloroharmine (6,8-diCl-Ha), thermal stability of chloroharmine derivatives under acidic and alkaline conditions, composition (% character) of relevant Molecular Orbitals of chloroharmine derivatives, experimental and calculated electronic spectra of 8-Cl-Ha and 8-Cl-HaH$^+$, 6,8-diCl-Ha and 6,8-diCl-HaH$^+$, evolution of the βCs and H_2O_2 concentrations in irradiated air-equilibrated aqueous solutions, comparative analysis of the effect of HCl and $HClO_4$ on the photodegradation of 6-Cl-HaH$^+$, triplet state kinetics, and evolution of the βCs and H_2O_2 concentrations in irradiated air-equilibrated aqueous solutions in the presence of ROS scavengers. See DOI: 10.1039/b000000x/

ACKNOWLEDGEMENTS

The present work was partially supported by CONICET (PIP 11220120100072CO), ANPCyT (PICT 2012-0423, 2013-2536 and 2014-2856), UBA (X088), UNSAM (E103), MinCyT-DAAD Cooperation Program (DA/11/15), DAAD (Equipment Grants for Higher Education and Comparable Scientific and Research Institutions in Developing Countries) and 3PA. FAORS and JGY thank CONICET for doctoral research fellowships. MMG, MPD, EW, REB and FMC are research members of CONICET. Authors deeply thank C. G. Alberici (CONICET) for his technical support, Dr. P. R. Ogilby for his contributions in singlet oxygen and laser flash photolysis experiments (performed at Center for Oxygen Microscopy and Imaging, University of Aarhus, Denmark) and Dr. B. Epe for his careful reading of the manuscript and for his invaluable editorial suggestions which greatly enhanced its quality.

REFERENCES AND NOTES

View Article Online
DOI: 10.1039/C5CP05866J

1. Susilo, R.; Rommelspacher, H. Naunyn-Schmiedeberg's Archives of Pharmacology 1987, 335(1), 70-76.
2. Spijkerman, R.; van den Eijnden, R.; van de Mheen, D.; Bongers, I.; Fekkes, D. Eur Neuropsychopharmacol 2002, 12(1), 61-71.
3. Torreilles, J.; Guerin, M. C.; Previero, A. Biochimie 1985, 67(9), 929-947.
4. Pfau, W.; Skog, K. Journal of Chromatography B: Analytical Technologies in the Biomedical and Life Sciences 2004, 802(1), 115-126.
5. Breyer-Pfaff, U.; Wiatr, G.; Stevens, I.; Jörg Gaertner, H.; Mundle, G.; Mann, K. Life Sciences 1996, 58(17), 1425-1432.
6. Kam, T.-S.; Sim, K.-M.; Koyano, T.; Komiyama, K. Phytochemistry 1999, 50(1), 75-79.
7. Hemmateenejad, B.; Abbaspour, A.; Maghami, H.; Miri, R.; Panjehshahin, M. R. Analytica Chimica Acta 2006, 575(2), 290-299.
8. Herraiz, T.; Galisteo, J. Journal of Agricultural and Food Chemistry 2003, 51(24), 7156-7161.
9. Stachell, S. J.; Stockwell, S. A.; Van Vranken, D. L. Chemistry & Biology 1999, 6(8), 531-539.
10. Siderhurst, M. S.; James, D. M.; Rithner, C. D.; Dick, D. L.; Bjostad, L. B. J Econ Entomol 2005, 98(5), 1669-1678.
11. Ramesh, S.; Rajan, R.; Santhanam, R. Freshwater Phytopharmaceutical Compounds, CRC Press, 2013; 250 p.
12. Davidson, B. S. Chemical Reviews 1993, 93(5), 1771-1791.
13. Dembitsky, V. M.; Tolostikov, G. A. Chemistry for Sustainable Development 2003, 11, 451-466.
14. Fattorusso, E.; Taglialatela-Scafati, O. Modern Alkaloids: Structure, Isolation, Synthesis, and Biology, Wiley, 2008; 689 p.
15. Rinehart, K. L.; Kobayashi, J.; Harbour, G. C.; Gilmore, J.; Mascal, M.; Holt, T. G.; Shield, L. S.; Lafargue, F. Journal of the American Chemical Society 1987, 109(11), 3378-3387.
16. Kobayashi, J.; Harbour, G. C.; Gilmore, J.; Rinehart, K. L. Journal of the American Chemical Society 1984, 106(5), 1526-1528.
17. Debitus, C.; Laurent, D.; Pais, M. Journal of Natural Products 1988, 51(4), 799-801.
18. Blunt, J. W.; Lake, R. J.; Munro, M. H. G.; Toyokuni, T. Tetrahedron Letters 1987, 28(16), 1825-1826.
19. Aiello, A.; Fattorusso, E.; Magno, S.; Mayol, L. Tetrahedron 1987, 43(24), 5929-5932.
20. Larsen, L. K.; Moore, R. E.; Patterson, G. M. L. Journal of Natural Products 1994, 57(3), 419-421.
21. Lake, R. J.; Brennan, M. M.; Blunt, J. W.; Munro, M. H. G.; Pannell, L. K. Tetrahedron Letters 1988, 29(18), 2255-2256.
22. Rashid, M. A.; Gustafson, K. R.; Boyd, M. R. Journal of Natural Products 2001, 64(11), 1454-1456.
23. Huber, K.; Brault, L.; Fedorov, O.; Gasser, C.; Filippakopoulos, P.; Bullock, A. N.; Fabbro, D.; Trappe, J.; Schwaller, J.; Knapp, S.; Bracher, F. Journal of Medicinal Chemistry 2012, 55(1), 403-413.
24. Gonzalez, M. M.; Pellon-Maison, M.; Ales-Gandolfo, M. A.; Gonzalez-Baró, M. R.; Erra-Balsells, R.; Cabrerizo, F. M. Organic and Biomolecular Chemistry 2010, 8(11), 2543-2552.
25. Gonzalez, M. M.; Vignoni, M.; Pellon-Maison, M.; Ales-Gandolfo, M. A.; Gonzalez-Baro, M. R.; Erra-Balsells, R.; Epe, B.; Cabrerizo, F. M. Organic and Biomolecular Chemistry 2012, 10(9), 1807-1819.
26. Gonzalez, M. M.; Rasse-Suriani, F. A. O.; Franca, C. A.; Pis Diez, R.; Gholipour, Y.; Nonami, H.; Erra-Balsells, R.; Cabrerizo, F. M. Organic and Biomolecular Chemistry 2012, 10, 9359-9372.
27. Vignoni, M.; Rasse-Suriani, F. A. O.; Butzbach, K.; Erra-Balsells, R.; Epe, B.; Cabrerizo, F. M. Organic & Biomolecular Chemistry 2013, 11(32), 5300-5309.
28. Vignoni, M.; Erra-Balsells, R.; Epe, B.; Cabrerizo, F. M. Journal of Photochemistry and Photobiology B: Biology 2014, 132(0), 66-71.
29. Gonzalez, M. M.; Denofrio, M. P.; Garcia Einschlag, F. S.; Franca, C. A.; Pis Diez, R.; Erra-Balsells, R.; Cabrerizo, F. M. Physical Chemistry Chemical Physics 2014, 16, 16547-16562.
30. Yañuk, J. G.; Alomar, M. L.; Gonzalez, M. M.; Simon, F.; Erra-Balsells, R.; Rafti, M.; Cabrerizo, F. M. Physical Chemistry Chemical Physics 2015, 17(19), 12462-12465.
31. Tarzi, O. I.; Ponce, M. A.; Cabrerizo, F. M.; Bonesi, S. M.; Erra-Balsells, R. Arkivoc 2005, (vii), 295-310.
32. Tarzi, O. I.; Erra-Balsells, R. Journal of Photochemistry and Photobiology B: Biology 2006, 82(2), 79-93.
33. Tarzi, O. I.; Erra-Balsells, R. Journal of Photochemistry and Photobiology B: Biology 2005, 80(1), 29-45.
34. Hrsak, D.; Holmegaard, L.; Poulsen, A. S.; List, N. H.; Kongsted, J.; Denofrio, M. P.; Erra-Balsells, R.; Cabrerizo, F. M.; Christiansen, O.; Ogilby, P. R. Physical Chemistry Chemical Physics 2015, 17(18), 12090-12099.
35. Gonzalez, M. M.; Salum, M. L.; Gholipour, Y.; Cabrerizo, F. M.; Erra-Balsells, R. Photochemical & Photobiological Sciences 2009, 8(8), 1139-1149.
36. Gonzalez, M. M.; Arnbjerg, J.; Paula Denofrio, M.; Erra-Balsells, R.; Ogilby, P. R.; Cabrerizo, F. M. Journal of Physical Chemistry A 2009, 113(24), 6648-6656.
37. Cabrerizo, F. M.; Arnbjerg, J.; Denofrio, M. P.; Erra-Balsells, R.; Ogilby, P. R. ChemPhysChem 2010, 11(4), 796-798.
38. Alomar, M. L.; Gonzalez, M. M.; Erra-Balsells, R.; Cabrerizo, F. M. Journal of Photochemistry and Photobiology B: Biology 2014(136), 26-27.
39. Ponce, M. A.; Tarzi, O. I.; Erra-Balsells, R. Journal of Heterocyclic Chemistry 2003, 40(3), 419-426.
40. Cabrerizo, F. M.; Thomas, A. H.; Lorente, C.; Dántola, M. L.; Petroselli, G.; Erra-Balsells, R.; Capparelli, A. L. Helvetica Chimica Acta 2004, 87(2), 349-365.
41. Braslavsky, S. E. Pure and Applied Chemistry 2007, 85(7), 1437-1449.
42. Cabrerizo, F. M.; Dantola, M. L.; Thomas, A. H.; Lorente, C.; Braun, A. M.; Oliveros, E.; Capparelli, A. L. Chemistry and Biodiversity 2004, 1(11), 1800-1811.
43. Thomas, A. H.; Cabrerizo, R.; Vignoni, M.; Erra-Balsells, R.; Cabrerizo, F. M.; Capparelli, A. L. Helvetica Chimica Acta 2006, 89(6), 1090-1104.
44. Meech, S. R.; Phillips, D. Journal of Photochemistry 1983, 23(2), 193-217.
45. Martí, C.; Jürgens, O.; Cuenca, O.; Casals, M.; Nonell, S. Journal of Photochemistry and Photobiology A: Chemistry 1996, 97(1â€“2), 11-18.
46. Arnbjerg, J.; Johnsen, M.; Frederiksen, P. K.; Braslavsky, S. E.; Ogilby, P. R. The Journal of Physical Chemistry A 2006, 110(23), 7375-7385.
47. Hohenberg, P.; Kohn, W. Phys Rev 1964, 136(3B), B864-B871.
48. Kohn, W.; Sham, L. J. Phys Rev 1965, 140(4A), A1133-A1138.
49. Parr, R. G.; Yang, W. Density Functional Theory of Atoms and Molecules, Oxford University Press, 1989.
50. Frisch, M. J.; Trucks, G. W.; Schlegel, H. B.; Scuseria, G. E.; Robb, M. A.; Cheeseman, J. R.; Scalmani, G.; Barone, V.; Mennucci, B.; Petersson, G. A.; Nakatsuji, H.; Caricato, M.; Li, X.; Hratchian, H. P.; Izmaylov, A. F.; Bloino, J.; Zheng, G.; Sonnenberg, J. L.; Hada, M.; Ehara, M.; Toyota, K.; Fukuda, R.; Hasegawa, J.; Ishida, M.; Nakajima, T.; Honda, Y.; Kitao, O.; Nakai, H.; Vreven, T.; J. A. Montgomery, J.; Peralta, J. E.; Ogliaro, F.; Bearpark, M.; Heyd, J. J.; Brothers, E.; Kudin, K. N.; Staroverov, V. N.; Keith, T.; Kobayashi, R.; Normand, J.; Raghavachari, K.; Rendell, A.; Burant, J. C.; Iyengar, S. S.; Tomasi, J.; Cossi, M.; Rega, N.; Millam, J. M.; Klene, M.; Knox, J. E.; Cross, J. B.; Bakken, V.; Adamo, C.; Jaramillo, J.; Gomperts, R.; Stratmann, R. E.; Yazyev, O.; Austin, A. J.; Cammi, R.; Pomelli, C.; Ochterski, J. W.; Martin, R. L.; Morokuma, K.; Zakrzewski, V. G.; Voth, G. A.; Salvador, P.; Dannenberg, J. J.; Dapprich, S.; Daniels, A. D.; Farkas, O.; Foresman, J. B.; Ortiz, J. V.; Cioslowski, J.; Fox, D. J. Gaussian 09, Revision A1, Gaussian, Inc Wallingford CT 2009.
51. Bauernschmitt, R.; Ahlrichs, R. Chem Phys Lett 1996, 256(4–5), 454-464.
52. Casida, M. E.; Jamorski, C.; Casida, K. C.; Salahub, D. R. J Chem Phys 1998, 108(11), 4439-4449.
53. Stratmann, R. E.; Scuseria, G. E.; Frisch, M. J. J Chem Phys 1998, 109(19), 8218-8224.
54. Barone, V.; Cossi, M. J Phys Chem A 1998, 102(11), 1995-2001.
55. Cossi, M.; Barone, V. J Chem Phys 2001, 115(10), 4708-4717.

View Article Online
DOI: 10.1039/C5CP05866J

56. Mennucci, B.; Tomasi, J. J Chem Phys 1997, 106(12), 5151-5158.
57. Gorelsky, S. I.; Lever, A. B. P. J Organomet Chem 2001, 635(1–2), 187-196.
58. Gorelsky, S. I. AOMix program, revision 681, http://wwwsg-chemnet/.
59. O'Boyle, N. GaussSum 225 program documentation (http://gausssumsourceforgenet/GaussSum_UVVis_Convolutionpdf).
60. Tomas Vert, F.; Zabala Sanchez, I.; Olba Torrent, A. Journal of Photochemistry 1983, 23(3), 355-368.
61. The small or null effect induced by the chlorine atom placed at C-8 described in (iii) and (iv) was suggested to be a consequence of the short distance between the chlorine atom and the pyrrolic NH group, leading place to the formation of a hydrogen-bridge-like-interaction. Thus, two opposite effects would operate simultaneously: a weak electron-donor effect (mesomeric effect) induced by the chlorine atom together with its spatial interaction with the hydrogen of the NH group by a hydrogen-bond-like interaction.
62. TD-DFT calculations do not produce "pure" H→L or H-1→L excitations as there is a mixing of around 80 - 90 % of the main excitation with 20-10% of the minor contribution.
63. This is in good agreement with the enhancemet on the basicity of the pyridinic nitrogen observed in excited bCs.
64. With the exception of 6,8-diCl-Ha (i.e., the neutral form) highly probable due to its fast chemical decomposition obseved under alkaline pH conditions.
65. Note that we have no direct evidence to further distinguish the zwitterionic from the anionic species. Although this, based on the literature, we will refer to this species as zwitterion (Z).
66. Turro, N. J., editor. Modern Molecular Photochemistry: Menlo Park, 1978.
67. Plummer, B. F.; Steffen, L. K.; Braley, T. L.; Reese, W. G.; Zych, K.; Van Dyke, G.; Tulley, B. Journal of the American Chemical Society 1993, 115(24), 11542-11551.
68. Varela, A. P.; Burrows, H. D.; Douglas, P.; da Graça Miguel, M. Journal of Photochemistry and Photobiology A: Chemistry 2001, 146(1-2), 29-36.
69. Becker, R. S.; Ferreira, L. F. V.; Elisei, F.; Machado, I.; Latterini, L. Photochemistry and Photobiology 2005, 81(5), 1195-1204.
70. Mesaros, M.; Tarzi, O. I.; Erra-Balsells, R.; Bilmes, G. M. Chemical Physics Letters 2006, 426(4-6), 334-340.
71. Note that, in aerated aqueous solutions, no transients with lifetimes in the microsencond to second timescale were observed by Varela *et. al.* This is in agreement to the fact that lifetimes of the transients in aerated solutions observed in this work are shorter than the excitation pulse used by these authors.
72. Wolfbeis, O. S.; Fuerlinger, E. Z Phys Chem (Wiesbaden) 1982, 129, 171-183.
73. Note that for 8-Cl-Ha and 6,8-diCl-Ha a similar set of experiments was not done due to the instability of these two chloroharmines in the time-window of the photochemical experiments.
74. Downum, K. R. New Phytologist 1992, 122(3), 401-420.
75. Mercader, A. G.; Duchowicz, P. R.; Fernández, F. M.; Castro, E. A.; Cabrerizo, F. M.; Thomas, A. H. Journal of Molecular Graphics and Modelling 2009, 28(1), 12-19.
76. Erra-Balsells, R.; Frasca, A. R. Tetrahedron 1983, 39, 33-39.
77. de Meester, C. Mutation Research/Reviews in Genetic Toxicology 1995, 339(3), 139-153.

View Article Online
DOI: 10.1039/C5CP05866J

GRAPHICAL ABSTRACT

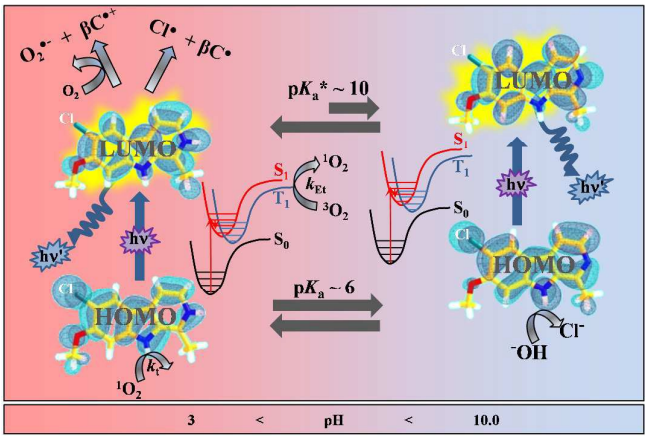

In water, chloroharmines follow very distinctive thermal and photochemical pH- and O_2-dependent-reaction pathways.